Optimal Transmitter Power Control for Indoor RGB-based Visible Light Communication

Christian Kamwangala

A dissertation submitted to the Faculty of Engineering and the Built Environment, University of the Witwatersrand, Johannesburg, in fulfilment of the requirements for the degree of Master of Science in Engineering.

Johannesburg, 05 October 2018

Declaration of Authorship

I, Christian KAMWANGALA, declare that this dissertation titled, "Optimal Transmitter Power Control for Indoor RGB-based Visible Light Communication" is my own, unaided work, except where otherwise acknowledged. It is being submitted for the degree of Master of Science in Engineering to the University of the Witwatersrand, Johannesburg. It has not been submitted before for any degree or examination to any other university.

Signed:

Date: 05 October 2018

"But everything exposed by the light becomes visible-and everything that is illuminated becomes a light."

– Ephesians 5:13

Abstract

Despite efforts to improve the efficiency and the spacial reuse of the ubiquitous RF frequencies range, the RF spectrum suffers from several issues, namely spectrum congestion and lack of bandwidth for future technologies such as 5G. Visible light communication (VLC) is a wireless technology that uses light as medium of communication. With light emitting diodes (LEDs) lighting becoming common, it is a natural extension of the lighting technology to modulate the LEDs at high speed to enable potentially high bandwidth downlinks.

Higher bandwidth becomes a major challenge in the development and implementation of VLC systems as transmission rates increase. One way of increasing bandwidth is through wavelength division multiplexing (WDM) in multicarrier systems that use red, green and blue (RGB) light emitting diodes to produce white light. However, these systems often suffer from low performance because of crosstalk interference, mainly caused by the imperfect nature of optical filters used to discriminate between the colours. The current research project aims to study the effects of optimal transmitter power control on the performance of WDM RGB-LEDs VLC systems. The research investigates both centralized and distributed scenarios, using the water-filling algorithm and the Refereed Game Theory to mitigate the interference between the different light colour carriers.

Results for the centralized power control show that by using mathematical models that take into consideration the effects of optical filters used for detection of colour signals, one is able to predict the trends in the overall system's performance. This enables us to adequately, determine the optimal power levels in the red and blue channels that result in the best overall performance of the system. This information is then used to formulate a distributed optimization power control scheme based on the Refereed Game Theory, which shows that cooperation between colour carriers to minimize crosstalk can be enforced by introducing a referee.

Acknowledgements

I would like to first thank God and the Virgin Mary for always being by my side through the ups and downs and giving me the strength to push through the tough times during the course of my research work.

Special thanks to my supervisor Prof. Ling Cheng for his amazing guidance throughout my research. I also thank my co-supervisor Mr. Mitchell Cox for his support and guidance throughout the course of my research. Thanks goes to my family for the constant emotional and monetary support provided throughout the course of my academic career which has led to the completion of this masters dissertation.

I would like to acknowledge the support of the Center for Telecommunications Access and Services (CeTAS) as well as the University of the Witwatersrand which have given their financial support to my research work.

I wish to convey my sincere thanks to my friends and members of the Optical Communication Laboratory Daniel Holmes, Shamin Achari, and Femi Kolade for their insight, assistance and words of encouragement throughout. I would also like to thank Mike De Gouveia for helping with the soldering of the hardware on the experimental setup used in this research.

Finally, I would not have made it through my masters if it was not for the support of every single amazing person in my life…

Contents

List of Figures

List of Tables

List of Abbreviations

ACO-OFDM	**A**symmetrically **C**lipped **O**ptical **O**rthogonal **F**requency **D**ivision **M**ultiplexing
ADC	**A**nalog to **D**igital **C**onverter
AWGN	**A**dditive **W**hite **G**aussian **N**oise
BER	**B**it **E**rror **R**ate
CAP	**C**arrier-less **A**mplitude and **P**hase
DCO-OFDM	**D**irect **C**urrent biased **O**ptical **O**rthogonal **F**requency **D**ivision **M**ultiplexing
DMT	**D**iscrete **M**ulti **T**one
IM/DD	**I**ntensity **M**odulation and **d**irect **d**etection
IOT	**I**nternet of **T**hings
LED	**L**ight **E**mitting **D**iode
LiFi	**Li**ght **Fi**delity
LOS	**L**ine **O**f **S**ight
MIMO	**M**ultiple **I**nput **M**ultiple **O**utput
NRZ-OOK	**N**on **R**eturn to **Z**ero **O**n **O**ff **K**eying
OFDM	**O**rthogonal **F**requency **D**ivision **M**ultiplexing
OOK	**O**n **O**ff **K**eying
OTD	**O**ptimal **T**hreshold **D**etection
PAM	**P**ulse **A**mplitude **M**odulated
PAM-DMT	**P**ulse **A**mplitude **M**odulated **D**iscrete **M**ulti **T**one
PWM	**P**ulse **FW**idth **M**odulation
RF	**R**adio **F**requency
RGB	**R**ed **G**reen **B**lue

SFSK	**S**pread **F**requency **S**hift **K**eying
SIFT	**S**cale **i**nvariant **F**eature **T**ransform
SNR	**S**ignal to **N**oise **R**atio
TIA	**T**rans **I**mpedance **A**mplifier
VLC	**V**isible **L**ight **C**ommunication
WDM	**W**avelength **D**ivision **M**ultiplexing

List of Symbols

$\mathbf{r}$	Column vector of received symbols
H	Transmission matrix
$\mathbf{s}$	Column vector of transmitted symbols
h_{rr}	Transmission coefficient of red light through red filter
h_{gg}	Transmission coefficient of green light through green filter
h_{bb}	Transmission coefficient of blue light through blue filter
P_o	Optical power
z_k	Unipolar symbols
T	Period of signal
V_{th}	Threshold voltage
$erfc$	Complementary error function
P_{avg}	Average radiant flux
σ_n^2	noise power
e	Optical to electrical conversion factor
C_{RGB}	Channel capacity for RGB VLC system
σ^2	noise variance
B	Transmission bandwidth
g^2	Channel gain
P_R	Optical power in the red channel
P_G	Optical power in the green channel
P_B	Optical power in the blue channel
$\mathcal{L}$	Lagrangian

λ	Lagrange multiplier
U	player payoffs
P_{ref}	Total power of the referee
P_i^{uplink}	uplink power

Resulting Publications

- **Kamwangala C.**, Cox M., and Cheng L., "Transmitter Power Control for a Multi-Carrier Visible Light Communication System", published in Wiley's Trans Emerging Tel Tech. 2018; e3453." https://doi.org/10.1002/ett.3453
- **Kamwangala C.**, Cox M., and Cheng L., "Distributed Transmitter Power Control for a Multi-Carrier Visible Light Communication System", to be submitted to IEEE Journal of Lightwave Technology.

Dedicated to my father, Pontien Kamwangala and my lovely late mother Betty Musau Kamwangala…

Chapter 1

Introduction

1.1 Problem Statement

Radio-based wireless communications are ubiquitous but suffer from several issues, namely, spectrum congestion and lack of bandwidth for future technologies such as 5G [1,2]. In addition, radio transmissions are difficult to secure because the signals easily penetrate through walls. Visible light communication (VLC) is a fast growing wireless technology which allows for data transmission through light as medium of communication. VLC systems use LEDs not only for lighting purposes, but also to transmit data, by modulating light at very high speeds that cannot be perceived by the human eye. The information is then recovered using a photosensitive device such as a camera or a photodiode [3–5].

With incandescent and fluorescent lamps being replaced by LEDs due to their high energy efficiency, the reuse of already existing lighting infrastructure for the simultaneous dual purpose of data transmission and illumination, suggests that VLC systems can be deployed with less effort and at lower costs [1,6].

1.2 The Research Problem

Ensuring efficient, high and reliable throughput in low-cost systems is the key to the deployment of VLC into a wide range of applications as an alternative high-speed wireless technology in future generation networks. Red, blue and green LEDs provide a more efficient use of the visible light bandwidth than white-light LEDs, and can be used to provide higher bandwidths in VLC systems. This can be accomplished through wavelength division multiplexing which is also used in fiber optic communication. However, discriminating between red, green and blue colour signals at the receiver often suffers from crosstalk interference due to the imperfect nature of optical filters used to filter out the unwanted wavelengths.

1.3 Research Question and Objectives

While most of the research in literature focus on more complex single colour LED modulation schemes such as OFDM and DMT [1, 7–10], the current research proposes to focus on improving the performance of indoor RGB-based multicarrier VLC systems, by applying *water-filling* and *Game Theory* power control techniques [11–17]. These methods work by efficiently allocating the available transmitter power between the different colour carriers, hence minimizing the crosstalk interference even though wideband optical filters are used. More specifically, the proposed work aims to answer the question:

What are the effects of optimal transmitter power control on the performance of an indoor, WDM-OOK modulated, RGB-based multicarrier VLC system, in terms of overall system BER?

In addition, the results generated through this research will also be applicable in high capacity systems which use narrowband optical filters.

The objectives of this research are:

- To study the nature of crosstalk interference in RGB-based OOK VLC systems.
- To develop a centralized power optimization approach for RGB-based VLC systems.
- To formulate a distributed power optimization approach for RGB-based VLC systems.
- Draw meaningful conclusions on the effects of transmitter power control in RGB-based VLC systems.

1.4 Research Methodology

For a communication channel that is corrupted by strong crosstalk interference, the adaptation of the transmitter signal to the channel conditions can improve the system's performance [11, 18]. However, for adaptation to be possible, the channel state should be available to the transmitter, usually by a channel estimation scheme or a reliable feedback mechanism [11]. This is the case with typical Li-Fi systems where channel state can be made available to the transmitter through the uplink feedback transmission.

The current research work can be broken up into two main phases: *Centralized power control* and *Distributed power control*. Figure 1.1 shows the major steps of the proposed methodology.

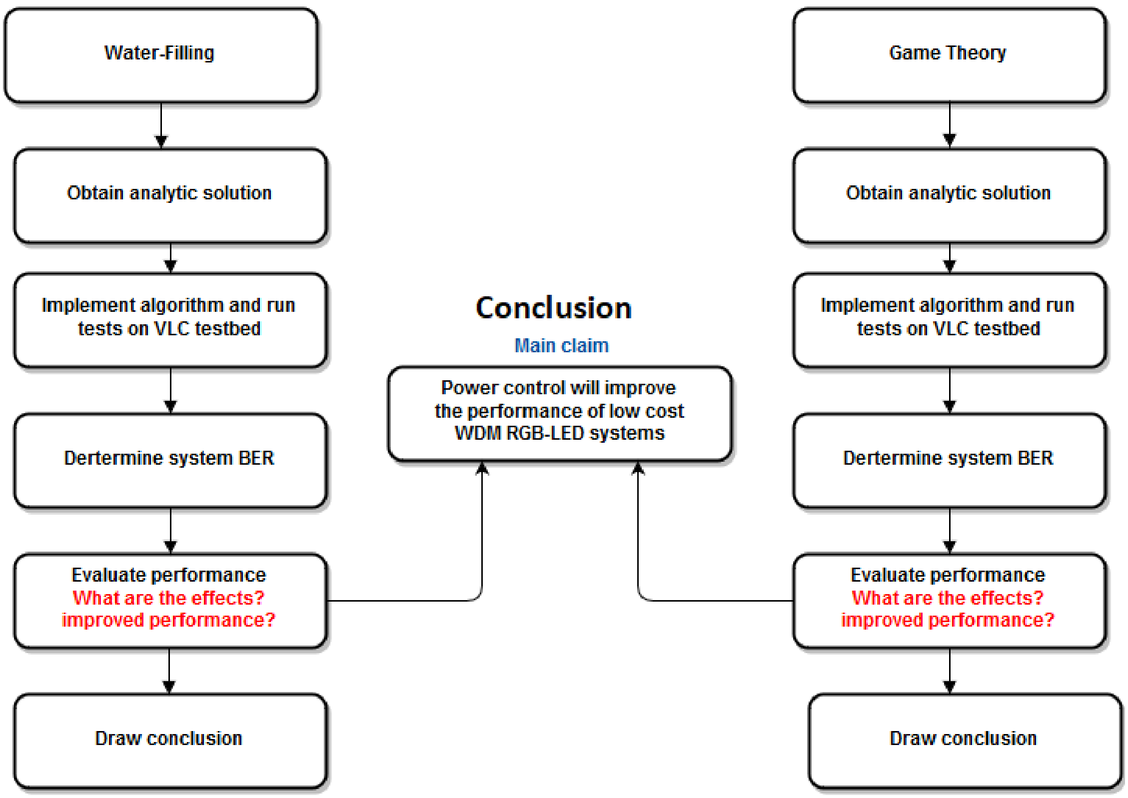

FIGURE 1.1: Research methodology.

1.5 Dissertation Organisation

To allow the reader a better understanding and flow of the research work, the remainder of this dissertation is outlined in this section with basic overview of the remaining chapters.

1.5.1 Chapter 2: Literature Review and Background

The current state of research in visible light communication as well as research on transmitter power control in VLC systems are presented in Chapter 2. Background information on data transmission schemes and dimming control techniques is also briefly discussed.

1.5.2 Chapter 3: A Water-filling Based Transmitter Power Control for a Multi-Carrier Visible Light Communication System

Chapter 3 focuses on developing the transmitter power control framework for the rest of the dissertation. Results from using a centralized power control scheme presented in this chapter, are based on the paper that has been published in the special issue of the Wiley's Transactions on Emerging Telecommunications Technologies [19]. In addition, the experimental testbed used for the collection of results in this work is also discussed.

1.5.3 Chapter 4: A Distributed Transmitter Power Control for Multi-Carrier Visible Light Communication System based on the Refereed Game Theory

Chapter 4 is dedicated to the formulation and implementation of a distributed power control scheme using the Refereed Game Theory. The Referee Game Theory is a branch of the broader field of Game Theory where the outcomes can be enforced by a third party entity known as the referee. The results presented in this chapter are to be submitted to an IEEE journal.

1.5.4 Chapter 5: Future Research and Conclusion

Chapter 5 concludes the research and provides a summary of the research presented along with recommendations for future work on the interference mitigation in multicarrier WDM VLC systems.

1.6 Summary

In this chapter, the main research idea has been presented in terms of the research problem, research questions and research objectives. The research methodology along with the layout for the remaining of this dissertation was also presented.

Chapter 2

Literature Review and Background

2.1 VLC Technology

Despite the best effort in improving the efficiency and spacial reuse of the ubiquitous RF frequencies range, the RF spectrum is proving scarce and expensive to accommodate growing traffic demand [3]. Compared to this, the optical spectrum consists of terahertz of unlicensed frequencies, equivalent up to 10 000 times more the entire RF spectrum that can be used for data transmission [1]. Li-Fi is a potential technology which uses visible light instead of radio waves for short range wireless communications [20–22].

The visible light spectrum ranges from 380 nm to 780 nm. These high frequencies mean that visible light cannot penetrate through most objects and walls. This inability of visible light signals to go through obstacles provides a security factor as potential eavesdroppers are required to be within the Line-Of-Sight (LOS) to intercept data transmissions.

Modulated visible light at high frequencies is completely safe for the human body and thus, poses no health risks as opposed to RF signals [23–26]. Visible light does not interfere with other radio wave signals and can be used in low interference-tolerant areas such as hospitals, aircrafts and nuclear power plants where traditional RF wireless systems can cause dangerous interference [27].

2.2 VLC Systems

A typical VLC system comprises a transmitter, a receiver and the optical channel as shown in Figure 2.1

FIGURE 2.1: Typical VLC system.

The transmitter in its simplest form consists of an LED which is used to transmit modulated data through an LED driver circuit. Two type of LEDs are often used in VLC systems namely, the single-colour LED and the multicolour LED.

- **Blue LED with Phosphor layer**: This is the most common way to produce white light in VLC systems. However, the yellow phosphor coating on the outside of the blue LED used to produce white light often limits the transmission bandwidth of these type of LEDs [2]. Using an analog RLC circuit for pre-equalization at the transmitter to compensate impedance matching of the LED, Yeh $et\ al.$ were able to increase the effective bandwidth of a phosphor LED from 1 MHz to approximately 12 MHz [28–30].

- **RGB LED**: White light can also be obtained through the combination of the three primary colours red, green and blue. RGB-LEDs are often used in multicarrier VLC systems where each colour represents a channel that can be modulated independently. Gigabits data rates using RGB-LEDs have been reported in literature [31–33].

The receiver is made of an optic detector and means for demodulating the received signal. The optic detector in a typical VLC system is a photodiode or a camera sensor. It has been reported in [7] that replacing a PIN photodiode with an avalanche photodiode can improve the performance of a VLC system. An example of a receiver that was designed by **C. Kamwangala** is shown in Figure 2.2

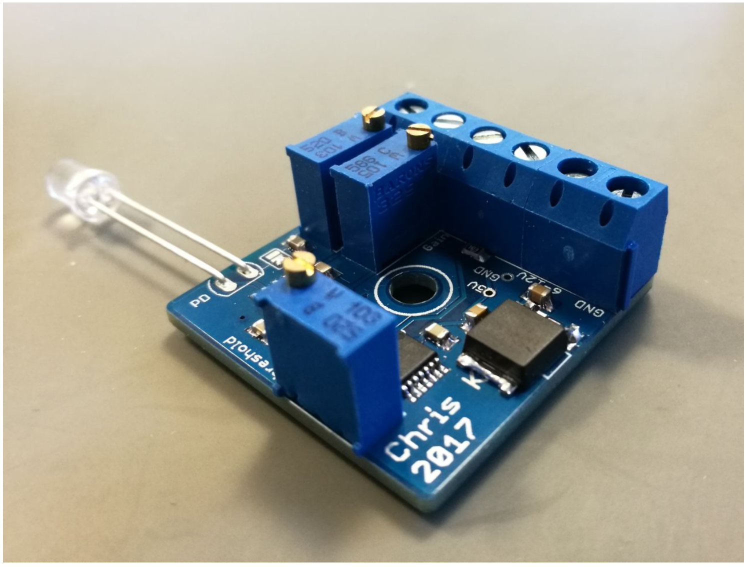

FIGURE 2.2: Single carrier OOK receiver based on OPA380 transimpedance amplifier.

For a VLC system with the additive white Gaussian noise channel, the transmission is governed by [34]

$$r = \mathrm{H}s + n \tag{2.1}$$

Where r and s represent the received and the transmitted symbols, respectively. H is the channel response and n denotes the channel noise. For VLC systems that use red, blue and green LEDs, the channel response H is represented by the matrix in (2.2)

$$\mathbf{r} = \mathrm{H}\mathbf{s} + \mathbf{n} = \begin{pmatrix} h_{rr} & h_{rg} & h_{rb} \\ h_{gr} & h_{gg} & h_{gb} \\ h_{br} & h_{bg} & h_{bb} \end{pmatrix} \mathbf{s} + \mathbf{n} \tag{2.2}$$

The diagonal entries h_{rr}, h_{gg}, and h_{bb} denote the interference free LOS link between a particular LED and its corresponding photodiode. The remaining entries represent the crosstalk between the channels.

2.3 On-Off Keying

Off-the-shelf LEDs emit an incoherent light beam which means that information can only be encoded in the intensity of the light [8]. Thus, it is impossible to modulate the amplitude or the phase of the light wave emitted by LEDs. This limits the implementation of VLC systems to intensity modulation and direct detection (IM/DD) systems [8]. However, subcarrier intensity modulation allows for more complex modulation schemes to be used. This is achieved by using an envelope detection on normal RF signals, superimposed onto the beam light [35].

Since IM/DD systems require the signal to be real-valued and non-negative, only a limited set of conventional modulation schemes can be adopted from the RF field and directly translated into VLC modulation schemes. This makes a simple modulation scheme such as OOK a suitable candidate for VLC, as it provides real signals that can be directly mapped to light intensity levels. As transmission rates increase, lower intensity levels in OOK can create a change in the emitted colour of LEDs, which can become an issue in lighting applications [1,36,37]. Nevertheless, using OOK as a proof of principle in the current research work is a good baseline for more complex modulation schemes.

OOK is a simple and widely used modulation scheme in which data bits ’1’ and ’0’ are represented by the on-state and the off-state of the LED, respectively. Although OOK is proven to be more sensitive to noise as compared to other single carrier schemes, enhanced schemes like OOK Non-Return-to-Zero have shown better noise rejection and highly improved data rates [38]. The signal waveform for NRZ-OOK is shown in Figure 2.3.

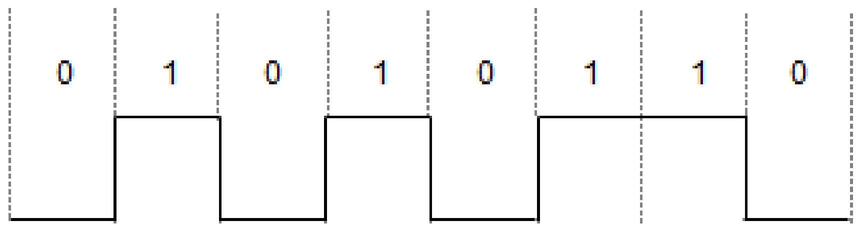

FIGURE 2.3: OOK modulation waveform.

NRZ-OOK can be expressed as

$$p(t) = P_o \cdot \sum_{q=-\infty}^{\infty} z_k \cdot rect\left(\frac{t - kT - T/2}{T}\right) \tag{2.3}$$

Where $z_k \in \{0, 1\}$ denotes the unipolar symbols that are transmitted, P_o is the optical power and T is the time required to transmit a symbol.

It is often necessary to be able to vary the level of lighting in a VLC system in order to accommodate different type of activities such as reading, sleeping and so on. A popular method for dimming the power of an LED to arbitrary levels is using Pulse Width Modulation (PWM). With PWM, the width of the pulses is adjusted to suit the desired level of dimming. It has been shown that any dimming level from 0% to 100% can be obtained with high PWM frequencies [37, 39–41].

Optimal Threshold Detection

The primary sensing device in a VLC system is often a photodiode. This photodiode converts the incoming optical signal into an electrical signal, by generating a current proportional to the light falling on the active area. The output current from the photodiode is then converted into a voltage signal using the transimpedance amplifier (TIA). The resulting voltage is fed to the ADC of the receiving device for decision-making and further processing.

For OOK, the decision of which bit was transmitted is based on the concept of Optimal Threshold Detection (OTD) which is illustrated in Figure 2.4. The decision whether a binary ′1′ or a binary ′0′ was sent is determined by the received voltage being above or below a predetermine threshold voltage V_{Th}.

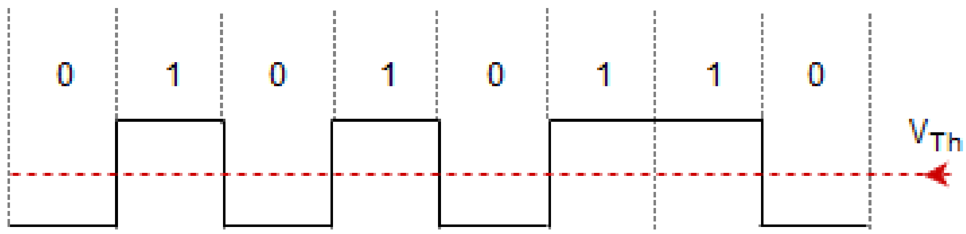

FIGURE 2.4: NRZ-OOK waveform with Optimal Threshold Detection.

The idea behind OTD is to determine the best possible threshold for the correct decoding of the incoming signal, with the lowest probability of making a bit decision error. OTD achieves this by placing the threshold level V_{Th} half-way between the levels representing the data bits ′1′ and ′0′, to ensure equally likely decoding probabilities for ′1s′ and ′0s′ data bits. This is also referred to as the maximum likelihood receiver, which minimizes the BER [42].

Bit Error Rate

As explained in the previous section, the received signal is sampled and compared to a threshold level to decide whether a data bit '1' or '0' was transmitted. However, due to shot noise, background noise and crosstalk at the receiver, errors may be introduced in determining which bit was transmitted.

The probability of error often referred to as BER, which is a function of the signal-to-noise ratio (SNR), is the most important metric used to assess the performance of a system in digital communication. Assuming that the channel model for an OOK modulated VLC system is AWGN, with only shot noise, and DC offset from the photodetector, therefore, as derived in [42], BER for OOK in an AWGN channel is given by (2.4)

$$BER_{OOK} = \frac{1}{2} erfc\left(\frac{i_s}{2\sqrt{2}\sigma_n}\right) = \frac{1}{2} erfc\left(\frac{SNR_0}{2\sqrt{2}}\right) \tag{2.4}$$

Where $erfc(x)$ is the complementary error function given as

$$erfc(x) = \frac{2}{\sqrt{\pi}} \int_{x}^{\infty} e^{-u^2} du \tag{2.5}$$

And

$$SNR_0 = \frac{(eP_{avg})^2}{\sigma_n^2} \tag{2.6}$$

P_{avg} is the average radiant flux emitted by the transmitter [W] and σ_n^2 is the noise power. The optical to electrical conversion factor e is assumed to be 1 without loss of generality.

2.4 Related Work and Techniques

There are several challenges facing VLC that need to be addressed, in order for VLC to be deployed into a wide range of indoor applications, as a high-speed wireless technology. As the transmission rates increase, channel capacity becomes a major challenge in achieving much higher transmission rates in VLC systems [2]. Different pre- and post-equalization techniques have been proposed to solve the channel capacity problem. Amongst the most notable solutions are OFDM, DMT and WDM. OFDM and DMT provide effective equalization in the frequency domain and make it possible to load data and energy adaptively in different subcarrier bands according to the channel's properties [7].

2.4.1 OFDM multicarrier VLC systems

Effective equalization can be enabled through OFDM with single-tap equalizers in the frequency domain. In addition, OFDM makes it possible to load data and energy adaptively in different subcarrier bands according to the channel's properties [7]. This results in a more efficient exploitation of the resources. Significant research has been conducted on OFDM-based VLC systems and reported in the literature [1, 8]. In [9], by implementing the DCO-OFDM transmission scheme, Afgani $et\ al.$ demonstrated for the first time a proof-of-concept for exploiting the high crest-factor of OFDM in VLC systems.

Using DCO-OFDM with bit and power loading and symmetric signal clipping, Vučić $et\ al.$ demonstrated a transmission rate of 500 Mbps [10]. The introduction of direct current biasing for the purpose of generating unipolar OFDM signals leads to an increase in power consumption, compared with traditional bipolar OFDM. To remedy to this problem, alternative methods for the generation of unipolar signals were investigated. This has resulted in the development of new inherently unipolar modulation techniques such as ACO-OFDM [43] and PAM-DMT [8].

In ACO-OFM [44], the negative parts of the OFDM frame are clipped to zero and only the odd-numbered subcarriers are modulated with information. The noise resulting from the clipping fall onto the even-numbered subcarriers and hence, it does not compromise the information in the OFDM frame [8]. It was shown in [43] that a similar concept can be used for PAM-DMT in order to produce non-negative signals. Contrary to ACO-OFDM, even-numbered and odd-numbered subcarriers can be used to transmit information, resulting in an improved performance. However, the clipping of the negative values in ACO-OFDM and PAM-DMT leads to an electrical energy penalty of 3 dB when compared to conventional bipolar OFDM [8].

Other variations of OFDM-based VLC systems such as, U-OFDM and Flip-OFDM have been proposed to further close the efficiency gap between the conventional bipolar OFDM and the optical OFDM. More information can be found in [8,45].

2.4.2 RGB multicarrier VLC systems

RGB LEDs have been proposed for multicarrier systems as a low-complexity WDM approach to increase the channel capacity of VLC systems [34]. Ideally, by modulating each colour dependently, the channel capacity of the system can be almost triple. However, this is not the case due to the high interference when wideband optical filters are used at the receiver.

The channel capacity for a single RGB-transmitter VLC system can therefore be written as

$$C_{RGB} = \sum_{i=1}^{3} \log_2 \left(1 + \frac{g^2 P_i}{\sigma^2 B} \right) \tag{2.7}$$

Where P_i is the transmit power in each colour channel and $P_i \in \{P_R, P_G, P_B\}$. σ^2 is the channel noise variance, and g is the channel gain. In the current work, the transmission bandwidth B in (2.7) is assumed to be 1 due to OOK being used for the modulation. The transmission of bit '1' makes use of the entire light bandwidth, while a '0' is transmitted in the absence of the bandwidth.

WDM RGB-VLC systems have been reported in literature [46–48]. In [49], Vučić $et\ al.$ demonstrated a 803 Mbit/s visible light WDM VLC system using a single RGB LED luminary at the transmitter, by employing optical filters at the receiver to discriminate between the different colours.

Wang $et\ al.$ have demonstrated a high-speed RGB-LED based WDM VLC system employing carrier-less amplitude and phase (CAP) modulation and recursive least square (RLS) based adaptive equalization [31]. They were able to achieve an aggregate data rate of 4.5Gb/s over a distance of 1.5 m in an indoor environment. In [50], the same group achieved 1.8 Gb/s data rate for a WDM VLC system over 50 m in outdoor environment, by using CAP modulation and receiver diversity technology.

Similar work was done in [32] where a novel PAM-8 modulation with phase shifted Manchester coding was proposed and experimentally demonstrated in an RGB-LED based WDM VLC system. An aggregated data rate of 3.375-Gb/s was achieved.

While most of the work on WDM RGB-LED VLC systems was focused on achieving high data rates, little has been done toward the mitigation of the high interference that systems with wideband optical filters suffer from. The most relevant work on interference mitigation in WDM RGB-LED VLC systems was reported in [51] and [52].

A colour filter free, multiple-input and multiple-output (MIMO) VLC system was presented in [52]. The system comprises a 3×3 RGB-LED array at the transmitter and a mobile phone camera sensor at the receiver to detect the incoming signals. OOK is used for the modulation and pulse width modulation (PWM) for adjusting the dimming level of each LED. In the proposed system, detection of incoming signals is done by using the camera sensor to record a 30 frames video of the transmitted signal. The feature matching method based on the scale-invariant feature transform (SIFT) [53] algorithm is then used to extract data from the processed video frames.

In [51], the author implemented a coded OOK modulation scheme based on spread frequency shift keying (Coded S-FSK), on a low-cost RGB-LED VLC system. A symbol mapping was developed in order to minimize the interference between the different colours as a result of wideband optical filters used at the receiver. A comparison between the conventional single colour OOK VLC system, the two colours scheme and the three colours scheme was conducted. We reported satisfactory results for the two colour schemes and an effective gain in data rate by a factor of 2.32 over conventional single colour OOK in the three colours scheme.

The objective of the current research project is to investigate the effects of optimal power control on interference mitigation in WDM RGB-LED VLC systems, for the purpose of improving the performance of such systems.

Crosstalk interference in a WDM RGB VLC system has a degrading effect on the overall performance of the system. The use of transmitter power control to reduce crosstalk interference between different channels has been a common practice in cellular radio systems over the years, and can be found in the literature [18]. The idea is to minimize the crosstalk interference at the receiver by adjusting the power of each carrier and maintain adequate transmission quality on the transmission link [18].

Various work on resources allocation schemes for VLC systems have been reported in literature [54]. However, most of these works have not considered any transmission coordination among the VLC transmitters. In [55], the average network delay in a hybrid RF and VLC system is minimized by selecting the optimal number of users to be hosted by a particular network. In [56], the max-min fairness throughput in a multi-user multi-input single-output VLC system is maximized under the optical power constraint by selecting an appropriate transmission strategy.

The most relevant work on coordinated interference management using power control in a VLC system is reported in [57]. The system under consideration comprises two transmitters and two receivers, and uses DCO-OFDM for the modulation scheme. The work focuses on maximizing a weighted additive utility function for two VLC communication pairs that share the whole bandwidth and transmit simultaneously. Each transmitter is able to change both its electrical signal power and the optical signal bias to maximize the utility function. Simulation results showed that the power control scheme could improve the performance of a VLC system under low interference.

In the current work, power control techniques will be applied to a WDM RGB-LED VLC system with wideband optical filters, in order to study the effects of coordinated interference management on the overall performance of such a system.

2.5 Summary

This chapter has given a background on the impact of VLC technology while also discussing the current state of research in visible light communication. A review of related work on transmitter power control specifically in VLC systems was also presented. In addition, the basic building blocks of VLC systems were also discussed together with the modulation scheme and dimming technique used in this research work.

Chapter 3

A Water Filling Based Transmitter Power Control for a Multi-Carrier Visible Light Communication System

Higher bandwidth becomes a major challenge in the development and implementation of visible light communication systems as transmission rates increase. One way of increasing bandwidth is through wavelength division multiplexing in multi-carrier systems that use red, green and blue light emitting diodes to produce white light. However, these systems often suffer from low performance as a result of crosstalk interference, mainly caused by the imperfect nature of optical filters used to discriminate between the colours. A centralized transmitter power control based on the water-filling algorithm is used to predict the trends in the performance of a multicarrier visible light communication system, that employs red and blue light emitting diodes.

This chapter presents the results of the special issue article which has been published in Wiley's Transactions on Emerging Telecommunications Technologies. The reference to the paper is currently the following as of 16/07/2018:

Kamwangala C., Cox MA., and Cheng L. "Transmitter power control for a multi-carrier visible light communication system. Trans Emerging Tel Tech. 2018;e3453." https://doi.org/10.1002/ett.3453

The main research idea was derived from a joint effort of **C. Kamwangala**, Prof. Ling Cheng and Mitchell. Cox. The software implementation used for data collection was coded in its entirety by **C. Kamwangala**. The experimental setup hardware was designed in collaboration with members of the **Wits Optical Communication Laboratory** and implemented by **C. Kamwangala**. The journal article was written by **C. Kamwangala** whilst Prof. Ling Cheng and Mitchel Cox supervised the research and ensured the journal article met the required quality standards for international publication.

3.1 Transmitter Power Control for RGB-based VLC Systems

The Internet of Things will rely heavily on wireless technologies but will cause major congestion on existing wireless infrastructure. LiFi is a potential technology which uses visible light instead of radio waves for short range wireless communications. With LED lighting becoming common, it is a natural extension of the lighting technology to modulate the LEDs at high speed to enable potentially high bandwidth downlinks [7–10, 43, 45].

In order to further increase the bandwidth of these so-called visible light communication (VLC) systems, wavelength division multiplexing (WDM), which is typically used in fiber optic communications, can be used. As white light can be produced using red, green, and blue (RGB) LEDs, it has been shown that multiplexing of these three colours leads to an increase in bandwidth [31,32,47,48,50,58]. Discriminating between the colours in a WDM system is imperfect and is the dominant source of crosstalk, which lowers the capacity of the system due to errors. In this work, we show theoretically and experimentally that a water-filling algorithm can be used to effectively combat this problem.

3.2 Coordinated Interference Management Techniques

Resource allocation and coordinated interference management techniques have proved effective in improving the performance of conventional radio communication systems specifically in cognitive radio systems, where systems are affected by high crosstalk interference [11–14, 18].

Application of coordinated interference and resource allocation management techniques such as bit-and-power algorithm to orthogonal frequency-division multiplexing VLC systems, have been reported in other works [54, 57, 59–62].

In this work, we use the water-filling approach to determine the power allocation for a WDM VLC system that employs red and blue LEDs. We are able to predict the trends in the system's bit error rate (BER) and use this information to locate the optimal power allocation point to ensure efficient use of the spectrum. This will result in an improved performance of the WDM system. The water-filling algorithm is a centralized optimization technique that allows for the adaptation of the transmitter signal to the channel condition to optimize channel capacity. This algorithm is commonly used in radio communication, when the channel is corrupted by strong crosstalk interference or severe fading to improve the transmission rate [11, 63]

In order to adapt this algorithm to the VLC channel, we propose and experimentally verify analytical expressions to determine the power allocation. The total optical power at the transmitter (the total intensity of the red and blue LEDs) is optimally shared between the red and blue subchannels, reducing crosstalk interference between these colour subchannels so as to minimize the overall system's BER. Our aim is to be able to find the optimal power allocation point and predict the trends in the overall system's BER, for different power allocations, and investigate how optical filters used at the receiver affect the location of this optimal point. This will enable the design and implementation of more efficient WDM VLC systems and further improve the performance of these VLC systems.

3.3 Channel Model for WDM RGB VLC Systems

In this section, we look at a multicarrier RGB VLC system and consider the main source of crosstalk in this type of systems. Consider a WDM RGB-LED VLC system with additive white Gaussian noise channel, as shown in Figure 3.1. The transmission is governed by (3.1) [34, 64]

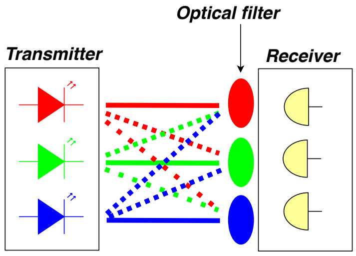

FIGURE 3.1: Graphical representation of a simple WDM multi-carrier RGB-LED VLC system corresponding to Equation 3.1.

$$\mathbf{r} = \mathrm{H}\mathbf{s} + \mathbf{n} = \begin{pmatrix} h_{rr} & h_{rg} & h_{rb} \\ h_{gr} & h_{gg} & h_{gb} \\ h_{br} & h_{bg} & h_{bb} \end{pmatrix} \mathbf{s} + \mathbf{n} \quad (3.1)$$

where H is the 3x3 channel transfer matrix and **n** is the 3x1 subchannel noise column vector. **r** and **s** are 3x1 column vectors that represent the received and transmitted symbols, respectively. The diagonal entries h_{rr}, h_{gg}, and h_{bb} denote the interference free line-of-sight link between a particular LED and its corresponding photodiode where the ideal value is one. The remaining entries represent the crosstalk between the different colour subchannels which are ideally zero.

Detection of RGB light signals at the receiver can be achieved using optical filters to prevent unwanted wavelengths from passing through, while allowing wavelengths of interest. Figure 3.2 depicts the frequency response obtained from a spectrometer of the different colour filters used on the implemented VLC system. Also shown in Figure 3.2 are the dominant wavelengths of the respective LEDs used.

As can be seen in Figure 3.2, the imperfect nature of the colour filters used at the receiver means that light from the green LED is able to go through the blue filter, while some red light will pass through the green and blue filters. The signal-to-noise ratio (SNR) in the received signal is dependent on both the shot (and other

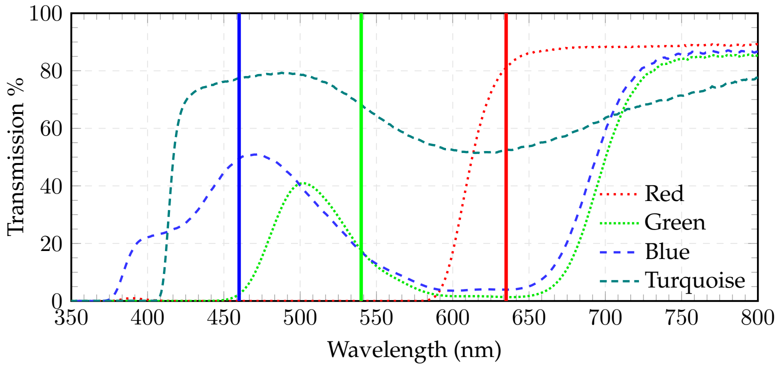

FIGURE 3.2: Spectrum of the colour filters and LEDs (vertical lines) used in the experiment. The wideband frequency response of the optical filters allows the various colour subchannels to interfere with each other, resulting in a poor overall system performance if optimal power control is not used.

electronically introduced) noise and background lighting. In this case, however, we assume that another contributor to the SNR is the crosstalk interference between subchannels. Put differently, due to the imperfect nature of the optical filters, each colour subchannel is directly affected by the interference from the other subchannels. Therefore, a more accurate expression for SNR should take into account the effects of the interference between the various colour subchannels. The SNR can be broken up into three separate expressions for each channel and written as

$$SNR_R = \frac{|h_{rr}|^2 P_R}{N_o + \Gamma_R}, \quad SNR_G = \frac{|h_{gg}|^2 P_G}{N_o + \Gamma_G} \quad \text{and} \quad SNR_B = \frac{|h_{bb}|^2 P_B}{N_o + \Gamma_B} \tag{3.2}$$

where P_i is the power of the respective LED, N_o is the normalized shot and background noise in the system, and Γ_i is the total interference from the other channels, given by

$$\begin{aligned} \Gamma_R &= |h_{rg}|^2 P_G + |h_{rb}|^2 P_B \\ \Gamma_G &= |h_{gr}|^2 P_R + |h_{gb}|^2 P_B \\ \Gamma_B &= |h_{br}|^2 P_R + |h_{bg}|^2 P_G. \end{aligned} \tag{3.3}$$

Equation (3.2) shows that the crosstalk interference between the colour subchannels increases with increasing transmit optical power. Increasing the total power does not necessarily improve the performance. The expressions for SNR in (3.2) also show that the interference between the different subchannels increases the total noise power of the system, which, in turn shifts the detection threshold level away from its optimal level, thus resulting in a reduced system performance.

The probability of error often referred to as BER is the most important metric used to assess the performance of a digital communication system. The BER is a function of the SNR and as OOK is the modulation scheme used in our VLC multicarrier system; the BER is expressed as [65,66]

$$\mathrm{BER}_{\mathrm{OOK}} = Q\left(\sqrt{\mathrm{SNR}}\right), \tag{3.4}$$

where $Q(x)$ is the Gaussian complementary error function. Assuming that the bit rate is the same across all colour subchannels, in an OOK modulated WDM VLC system with RGB LEDs, the overall BER can be expressed in terms of the individual BER in the red, blue and green subchannels as

$$\mathrm{BER}_{RGB} = \frac{1}{3}\left(\mathrm{BER}_R + \mathrm{BER}_G + \mathrm{BER}_B\right) \tag{3.5}$$

The variables BER_R, BER_B and BER_G in (3.5), represent the individual BER for the red, blue and green colour subchannels, respectively. The expression for the overall system's BER in (3.5) can now be written in terms of the Q-function in (3.4) and the SNR in (3.2) as

$$\mathrm{BER}_{RGB} = \frac{1}{3}\left(Q\left(\sqrt{\frac{|h_{rr}|^2 P_R}{N_o + \Gamma_R}}\right) + Q\left(\sqrt{\frac{|h_{gg}|^2 P_G}{N_o + \Gamma_G}}\right) + Q\left(\sqrt{\frac{|h_{bb}|^2 P_B}{N_o + \Gamma_B}}\right)\right) \tag{3.6}$$

From (3.6), it is clear that the crosstalk between the colour subchannels affects the overall system's BER. Therefore, the use of optimal power control to efficiently allocate the total power at the transmitter to reduce the crosstalk can greatly impact on the performance of the system, which is directly related to the system's BER.

3.4 Water-filling Optimal Power Control

The available optical power at the transmitter is constrained in an indoor VLC system, due to human eye safety concerns, flickering mitigation, and efforts to reduce power consumption. Various dimming techniques have been proposed to achieve different levels of illuminance when performing different types of activities [1]. In this project, PWM dimming control has been adopted for varying the power levels in the various color subchannels due to its ease of implementation.

Let P_{tot} denotes the total available optical power at the transmitter, then the power constraint in a WDM RGB-LED VLC system can be written as $P_{tot} = P_R + P_G + P_B$, where P_R, P_G and P_B are the respective optical power of the RGB channels. As can be seen in (3.2), the SNR of each colour subchannel is affected by the crosstalk interference from the other two colour subchannels, which, in turn, is a function of the allocated power in those two channels. Therefore, by efficiently allocating the available optical power at the transmitter and taking into consideration the SNR of the individual channel, the level of interference between the three subchannels (RGB) can be reduced, hence improving the overall performance of the system. When information about the state of the channel is available and if the channel can be divided into parallel independent subchannels such as in the WDM RGB-VLC, the problem of finding the optimal power allocation can be solved by the water-filling algorithm [11–14]. In the water-filling optimization, each subchannel represents a container that is filled with a certain amount from the total available power considering both noise and interference in the channel.

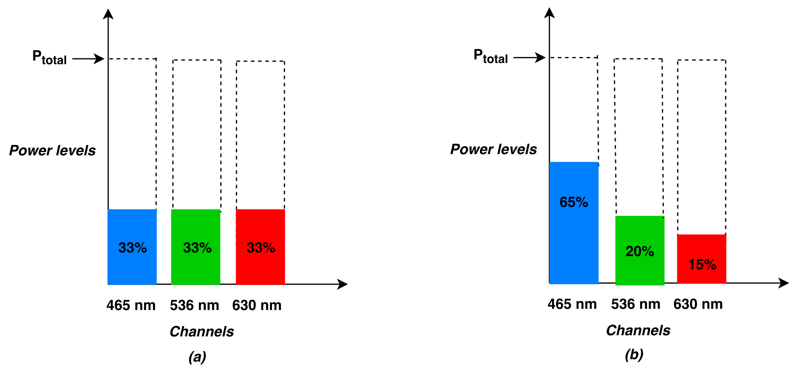

FIGURE 3.3: An example to illustrate the water-filling power control algorithm for a multicarrier red, green, and blue light-emitting diode visible light communication system. Each color subchannel is viewed as a container and the power levels are determined based on noise and interference to improve overall system performance. Recall from Figure 3.2 that we have a "bad" blue filter, which allows signals from the green and red subchannels to pass through. In case (a), equal power is allocated to all three subchannels, this creates a lot of crosstalk on the blue subchannel. In case (b), water-filling transmitter power control is used to find the optimal power allocation, which results in better overall system's performance. This results in an improved performance for the overall system.

To better understand how the water-filling algorithm will work in a WDM VLC system, consider the two scenarios in Figure 3.3. In the first scenario (see Figure 3.3a), the blue optical filter has a frequency response that allows a large amount of green and red lights to pass through. When transmitter power control is not being used, equal power is allocated to all three subchannels. This creates a lot of crosstalk on the blue subchannel and has a degrading effect on the overall performance of the system. Recall from (3.2) in Section 3.3 that the effect of crosstalk in a particular subchannel, is dependent on the amount of power in the other two subchannels.

In the second scenario (see Figure 3.3b), since the red and green optical optical filters are relatively "good" at keeping out the unwanted signals from the blue LED, we can remedy the effect of crosstalk by taking some power from the red and green subchannels and allocating more power to the blue LED to increase the signal-to-noise ratio in the blue subchannel, while at the same time reducing the amount of crosstalk contributed by the green and red subchannels without affecting too much the performance in these two subchannels. This results in a better performance in the blue subchannel and hence an improved overall system's performance.

The water-filling algorithm is usually formulated in terms of channel capacity. However, channel capacity cannot be directly measured in practice. This requires a different formulation that makes use of BER to assess the improvement made to the system. Assuming that the bit rate is the same across all color subchannels, the power allocation problem can be chosen so as to minimize the rate in (3.6). Under the power constraint that P_{tot} is a constant, the power allocation problem can be solved by finding the solution to the optimization problem in (3.7)

$$\text{minimize}\left[\frac{1}{3}\left(Q\left(\sqrt{\frac{|h_{rr}|^2 P_R}{N_o+\Gamma_R}}\right)+Q\left(\sqrt{\frac{|h_{gg}|^2 P_G}{N_o+\Gamma_G}}\right)+Q\left(\sqrt{\frac{|h_{bb}|^2 P_B}{N_o+\Gamma_B}}\right)\right)\right] \tag{3.7}$$

subject to

$$P_R + P_G + P_B = P_{tot} \quad \text{and} \quad P_R,\ P_G,\ P_B\ \geq 0 \tag{3.8}$$

The objective function in (3.7) is a convex function in the powers and as explained by [12], the solution to the optimization problem can be solved by the Lagrangian method. Consider the following expression:

$$\mathcal{L}(\lambda, P_R, P_G, P_B) \coloneqq \mathrm{BER_{RGB}} - \lambda(P_R + P_G + P_B) \tag{3.9}$$

where λ is the Lagrange multiplier, and $\mathrm{BER_{RGB}}$ is the overall BER of the system as defined in (3.6). Assuming P_i is the transmit power in each colour subchannel, the Kuhn-Tucker condition for optimal solution is

$$\left.\begin{aligned} \frac{\partial \mathcal{L}}{\partial P_i} &= 0 \; if \; P_i \geq 0 \\ \\ \frac{\partial \mathcal{L}}{\partial P_i} &\leq 0 \; if \; P_i = 0 \end{aligned}\right\} \quad \text{where} \quad P_i \in \{P_R, P_G, P_B\} \tag{3.10}$$

Using the expression for SNR given in (3.2), the general form of the power allocation for each channel can be expressed as

$$P_R = \frac{1}{\lambda} - \frac{N_o + \Gamma_R}{|h_{rr}|^2}, \quad P_G = \frac{1}{\lambda} - \frac{N_o + \Gamma_G}{|h_{gg}|^2} \quad \text{and} \quad P_B = \frac{1}{\lambda} - \frac{N_o + \Gamma_B}{|h_{bb}|^2} \tag{3.11}$$

where Γ_i is the total interference from the other channels in the respective channels defined in (3.4). The above expression is the optimal solution if the Lagrange multiplier λ satisfies the condition

$$\left(\frac{1}{\lambda} - \frac{N_o + \Gamma_R}{|h_{rr}|^2}\right) + \left(\frac{1}{\lambda} - \frac{N_o + \Gamma_G}{|h_{gg}|^2}\right) + \left(\frac{1}{\lambda} - \frac{N_o + \Gamma_B}{|h_{bb}|^2}\right) = P_{tot} \tag{3.12}$$

The inverse of the Lagrange multiplier can be regarded as a water level. Once the solution to (3.7) has been obtained, it will determine these water levels (see Figure 3.3) for the optimal power allocation. This can then be used to improve the performance of multicarrier WDM VLC systems.

In the next section, we are going to formulate an analytical solution to the optimization problem for a two channels WDM VLC system that employs red and blue LEDs and uses OOK as the modulation scheme.

3.4.1 Solution to optimization problem

In this work, we will consider a general scenario with two colours. The results obtained here can be generalized for application to three colours scheme or any number of wavelengths in WDM VLC systems. In the first part of this section, we look at a VLC system with two colour subchannels where there are no optical filters used to discriminate between the wavelengths. We then look at a more realistic scenario where the effect of the optical filters frequency response on the attenuation of the received signals is taken into consideration.

3.4.2 Case 1: Normalized channel attenuations

Consider a case where there are no optical filters used at the receiver; all colour subchannels attenuations are normalized and the system noise is uniform across all subchannels. Now consider a WDM VLC system with two colour subchannels, say red and blue. Let the total power in the system $P = P_R + P_B$ be a constant and the bit rate be the same across the two colour subchannels. The objective is to

$$\text{minimize} \quad \left[\frac{Q\left(\sqrt{\frac{P_R}{P-P_R+N_o}}\right) + Q\left(\sqrt{\frac{P-P_R}{P_R+N_o}}\right)}{2}\right] \tag{3.13}$$

where Q is the Gaussian Q-function defined in Equation (3.4) and $P_B = P - P_R$. The Gaussian Q-function can be approximated using the CDS approximation as described in the work of Chiani et al [65] and Chen and Beaulieu [66]

$$Q(x) \approx \frac{1}{12}\exp\left(-\frac{x^2}{2}\right) + \frac{1}{4}\exp\left(-\frac{2x^2}{3}\right). \tag{3.14}$$

Using the expression for the Q-function in (3.14) and substituting this into (3.13), a solution to the optimization problem can be found by taking the partial derivative with respect to P_R and equating the result to zero

$$\frac{\partial}{\partial P_R}\left(\frac{1}{12}\exp\left(-\frac{P_R}{2(P-P_R+N_o)}\right) + \frac{1}{4}\exp\left(-\frac{2P_R}{3(P-P_R+N_o)}\right)\right.$$

$$\left. + \frac{1}{12}\exp\left(-\frac{P-P_R}{2(P_R+N_o)}\right) + \frac{1}{4}\exp\left(-\frac{2(P-P_R)}{3(P_R+N_o)}\right)\right) = 0 \tag{3.15}$$

Solving for (3.15) yields the following results:

$$\frac{-P-N_o}{24(P-P_R+N_o)^2}\exp\left(\frac{-P_R}{2(P-P_R+N_o)}\right)+\frac{P+N_o}{24(P_R+N_o)^2}\exp\left(\frac{-P+P_R}{2(P_R+N_o)}\right)$$

$$\frac{-P-N_o}{6(P-P_R+N_o)^2}\exp\left(\frac{-2P_R}{3(P-P_R+N_o)}\right)+\frac{P+N_o}{6(P_R+N_o)^2}\exp\left(-\frac{2(P-P_R)}{3(P_R+N_o)}\right)=0 \tag{3.16}$$

Equation (3.16) shows that one of the stationary point for the cost function in (3.13) occurs when $P_R = P_B$, ie, when the total available power P is shared equally between the two color subchannels. However, this scenario results in the worst possible BER.

The aforementioned claims can be verified by plotting the cost function in (3.13) as a function of both P_R and P_B under total power P constraint as illustrated in Figure 3.4.

From Figure 3.4, one can see that there exist two other stationary points close to the two extremities. These are global minimums and they dictate that, to achieve a better overall BER performance in the system, more power must be allocated to one of the subchannels with respect to the other. This is equivalent in practice to using a single subchannel for data transmission. However, this is an extreme case as it is assumed that no optical filters were used at the receiver to discriminate between the different wavelengths.

Most of the work in literature on VLC systems which use WDM to increase the channel capacity, do not consider the effects of the type of filters used on the performance of such systems. In the next section, we investigate how the type of filters used affect the overall system's performance with respect to the power allocation in the different colour subchannels.

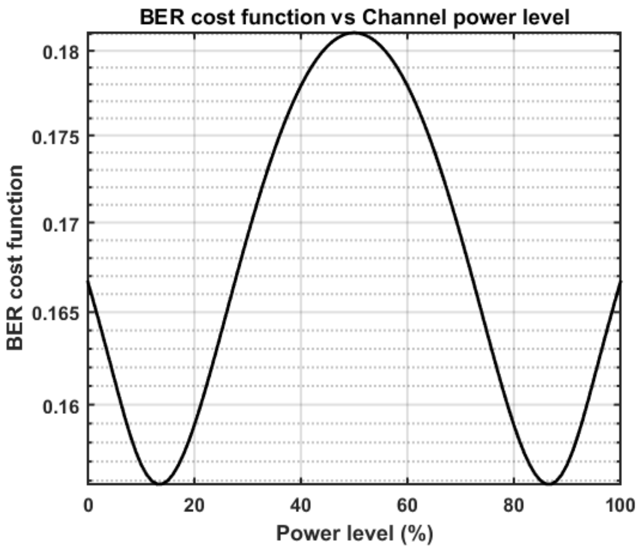

FIGURE 3.4: Simulated bit-error-rate (BER) cost function as a function of the power levels in the red and blue subchannels with normalized channel attenuations. The two plots are symmetrical and overlay each other. Equal power to the subchannels results in the worst performance at a global maximum, while better performances occur at global minimums close to the extremities where much more power is given to a single subchannel.

3.4.3 Case 2: Considering the effects of optical filters

Until now, we have considered an ideal scenario where the respective channel attenuations from the filters have been neglected. In practice, however, detection of RGB signals at the receiver requires using either optical colour filters or colour sensors. Optical colour filters have an absorption coefficient, which affect the SNR of the received signals, and hence results in signal attenuation. The optimization equation can now be written as

$$\text{minimize} \quad \left[\frac{Q\left(\sqrt{\frac{h_{rr}P_R}{h_{rb}(P-P_R)+N_o}}\right) + Q\left(\sqrt{\frac{h_{bb}(P-P_R)}{h_{br}P_R+N_o}}\right)}{2} \right], \tag{3.17}$$

where the h_{xx} variables represent entries in the transmission matrix H, such as that defined in (3.1). These absorption coefficients affect the shape of the cost function in (3.17), and hence determine the performance of the system for different type of power levels applied to the system. The effects of the absorption coefficients can be observed by looking at Figure 3.5 below.

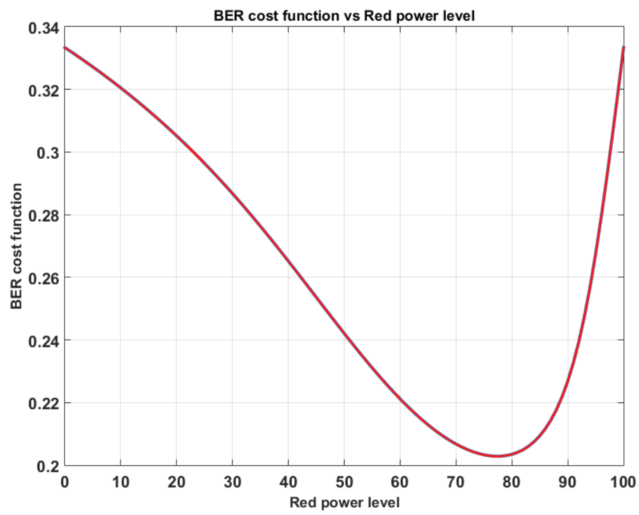

FIGURE 3.5: Simulated bit-error-rate (BER) cost function as a function of the power levels in the red and blue subchannels when taking into consideration the absorption coefficients of optical filters used at the receiver. This figure illustrates how these coefficients shape the objective function and dictate the power allocation in the system.

The inclusion of absorption coefficients in the optimization function in (3.17) results in added complexity when solving the problem analytically. However, a solution to the optimization problem can still be found through simulations of the objective function for the set of optical filters used in our experimental setup, and this solution is presented in the next section.

3.4.4 Simulation results

In order to better understand how the absorption coefficients affect the optimization cost function in (3.17), simulations were performed by substituting in the values for h_{rr}, h_{bb}, h_{rb} and h_{br} as measured for the filters used in the experiment. As an example of a low crosstalk case, the resulting H matrix for a two-color scheme using red and blue filters from Figure 3.2 is shown in (3.18) below

$$\mathrm{H} = \begin{pmatrix} 0.96 & 0.10 \\ 0.16 & 0.88 \end{pmatrix}. \tag{3.18}$$

It is important to note that as with the previous case, the channel's noise was assumed to be additive white Gaussian noise and has been normalized in the computer simulations. The resulting cost function with respect to the power allocation in the red and blue color subchannels is shown in Figure 3.6.

The values used for h_{rr}, h_{bb}, h_{rb} and h_{br} in the cost function of (3.17) are simply those of the optical filters used in our experimental setup, which can be read from Figure 3.2. Figure 3.6 shows the calculated values for "good" filters, namely, the blue and red, which have minimal crosstalk.

Taking a closer look at the plot in Figure 3.6 reveals that the optimal power allocation in this case is asymmetrical and does not lie half way between the two color subchannels as would be the case in a naive implementation. That said, because good filters have been used, the allocation is expected to be close to 50%. When higher crosstalk is present, the split will be more significant as shown in the experiment. The calculated optimal power settings are 57% of the total transmitter power for the blue subchannel, while the remaining 43% should be allocated to the red subchannel.

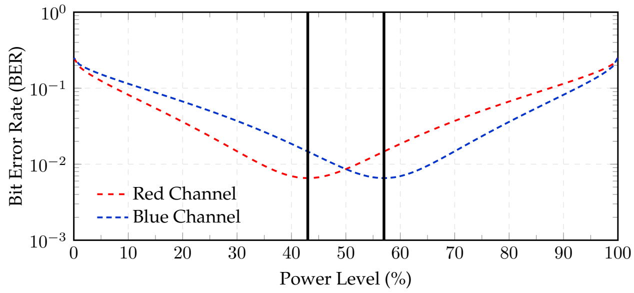

FIGURE 3.6: Bit-error-rate cost function to illustrate the trend in the system's overall performance as a function of the power allocation in the red and blue channels. This plot shows that the optimal power allocation point lies at 43% for the red subchannel and 57% for the blue. The channel noise was assumed to be additive white Gaussian noise and has been normalized for the simulation. Due to the fact that the total available power in the system is constrained, the two graphs are mirror images of each other in the vertical axis.

3.5 Experimental setup

The experimental setup of the WDM VLC testbed used in this research work with red and blue LEDs using modulating data over a distance of 1m optical channel is shown in Figure 3.7. Our WDM system comprises of discrete red and blue LEDs with wavelength in the regions of 630 nm (red) and 465 nm (blue). The downlink is the forward channel from the transmitters to the receiver used for data transmission, while the uplink in Figure 3.7 is the feedback channel from the receiver to the transmitters. This feedback is used to obtain information about the state of the channel and was implemented in software as a way to simulate a two-way system.

The Cree XLamp XB-D LEDs series was selected. These 3000 mW Radiant Flux LEDs show a high efficiency of up to 136 lumen/W in cool white(at 85° C, 350 mA), providing a nominal flux of 139 lumen at 25° C. With a maximum driving current of 1 A and a wide viewing angle from 115° to 140°, this is sufficient for data transfer over a distance of 1 m. Modulation bandwidth tests were conducted to assess the switching capability of the LEDs using a square wave. The tests show that no distortion occurs up to a frequency of 1 MHz transistor-transistor logic signal input.

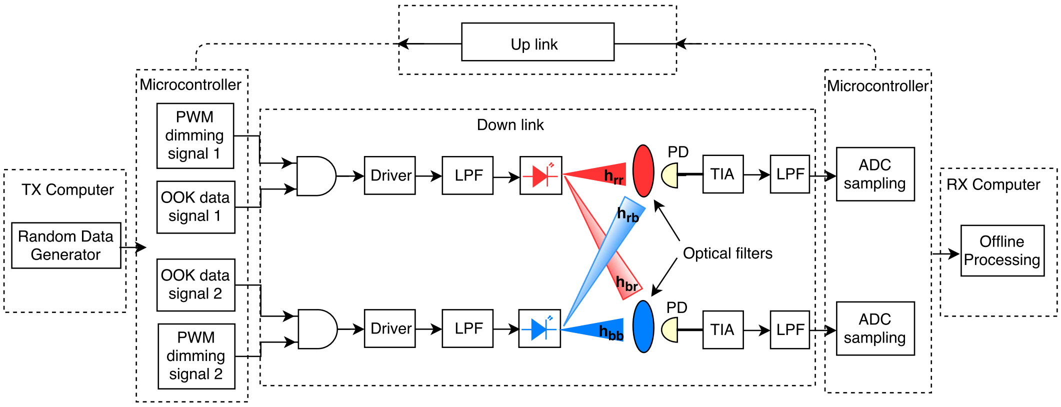

FIGURE 3.7: Block diagram of the experimental setup for the wavelength division multiplexing visible light communication system. The uplink feedback is used to obtain information about the state of the channel and was implemented in software as a way to simulate a two-way system. ADC, analog-to-digital converter; LPF: low pass filter; OOK, on off keying; PD: photodiode; PWM, pulse width modulation, TIA: transimpedance amplifier.

3.5.1 Transmitter

The main components of the transmitter are shown in Figure 3.8. The transmitter comprises of three OOK modulated channel carriers namely, red, green and blue. Each channel consists of a high luminance LED, a voltage controlled MOSFET driver, and a microcontroller unit responsible for generating the data signal that is sourced into the input of the LED driver circuit.

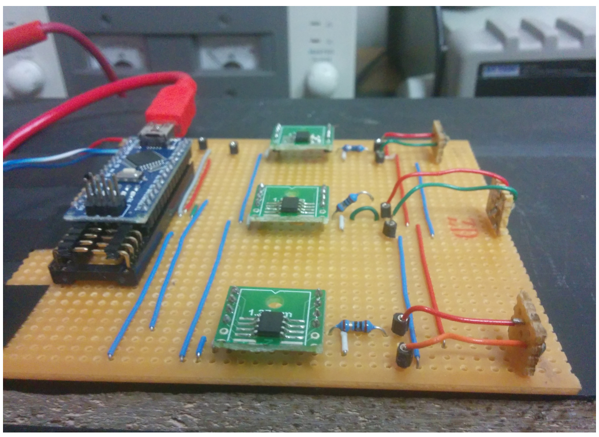

FIGURE 3.8: VLC OOK RGB transmitter

The corresponding circuit diagram for the transmitter is shown in Figure 3.9

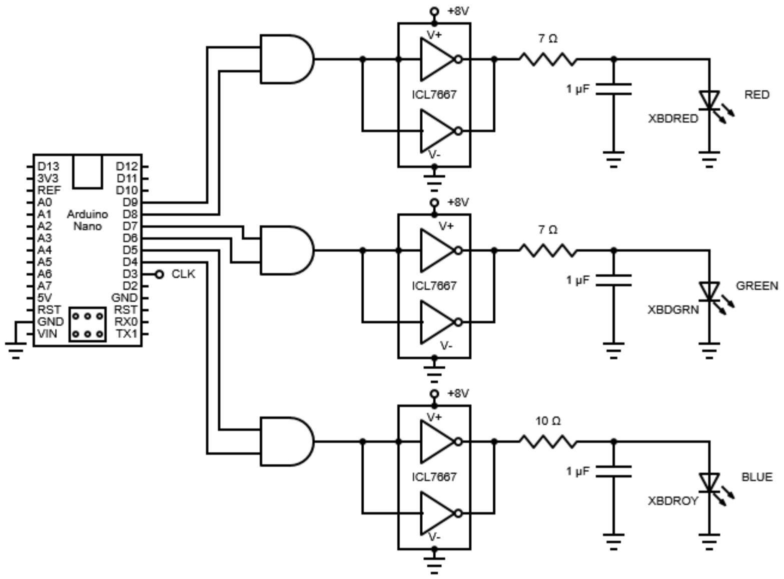

FIGURE 3.9: VLC OOK RGB transmitter circuit diagram

The data signals are generated from a computer and fed to a microcontroller unit to drive the two LEDs (red and blue) simultaneously and with the same bit rate. Two independent pulse-width-modulation dimming control signals are also generated by the microcontroller and combined with the data signals to vary the power allocated to each colour subchannel. The resulting signals are then used to modulate the LEDs.

3.5.2 Receiver

At the receiver (see Figure 3.10), optical colour filters are used to separate the incoming signals which are detected using a PIN photodiode with spectral range of sensitivity in the region of 400 nm to 1100 nm. This covers the LEDs used in this project with an active area of 1 mm^2. By use of a transimpedance amplifier, the output current from the photodiode is converted into a voltage signal that can be sampled by the analog-to-digital converter of the microcontroller. The resulting digital data is then fed to the receiving computer for BER analysis and further processing.

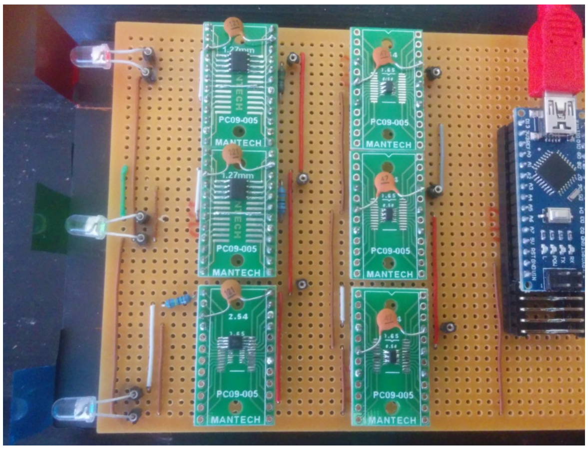

FIGURE 3.10: VLC OOK RGB receiver

The corresponding circuit diagram for the receiver is shown in Figure 3.11. The

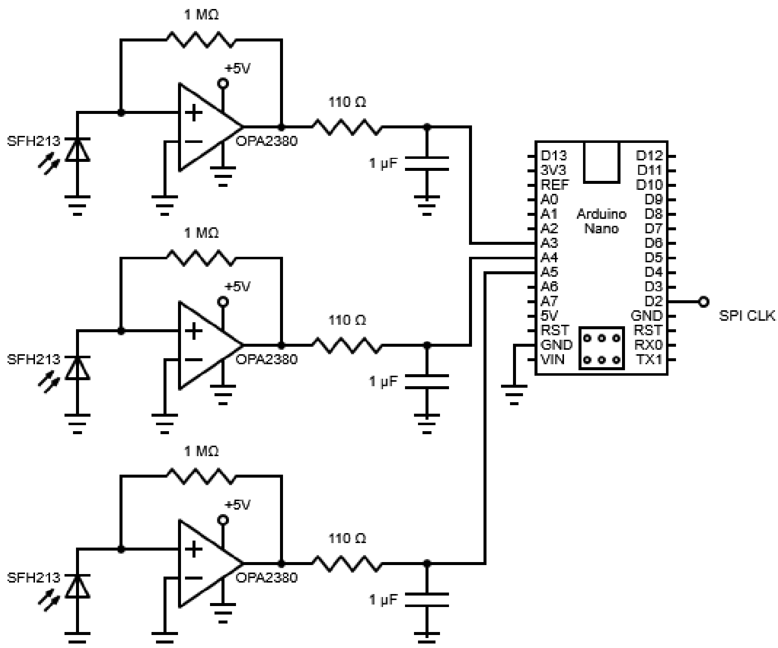

FIGURE 3.11: VLC OOK RGB receiver circuit diagram

uplink feedback from the receiver to the transmitter is used to obtain information about the state of the channel in the form of BER related to the h_{xx} values, when different type of filters are used at the receiver. This BER is then used to determine the optimal power allocation for the specific type of filters currently used in the system. In this project, the feedback channel was implemented in software as a way to simulate a two-way communication system on the experimental setup.

3.5.3 Transmit power control circuit

To experimentally verify the simulation results from Section 3.4.4 and be able to allocate the correct amount of optical power to the individual colour channels, requires the implementation of dimming control on the current VLC testbed. The IEEE 802.15.7 standard specifies several techniques for implementing dimming control in VLC systems based on the type of modulation scheme used [37,39–41,67].

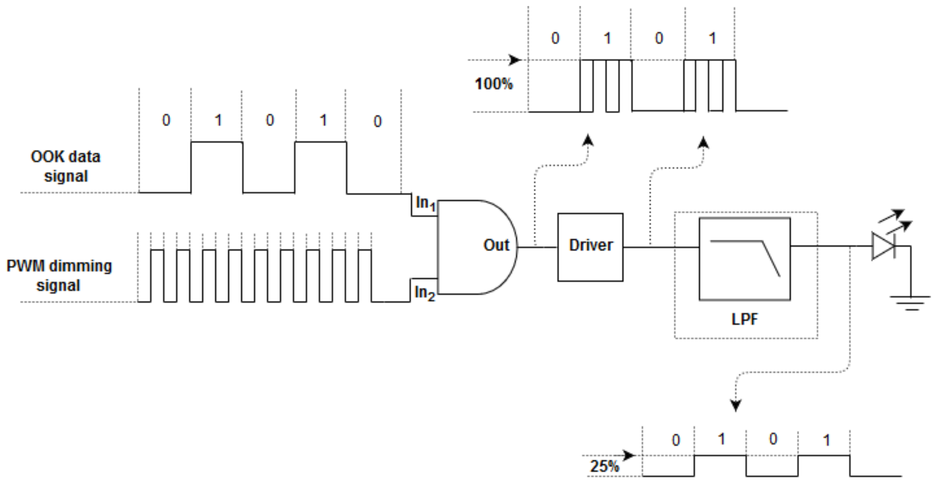

FIGURE 3.12: PWM dimming control

Pulse width modulation (PWM) dimming approach has been implemented in the current work (see Figure 3.12). The idea is to superimpose a high frequency PWM signal on top of the slower NRZ-OOK data signal, and then use a low-pass filter to obtain the required dimming of the data signal. The dimming level is control by the duty cycle of the high frequency PWM.

Due to the introduction of the high frequency PWM signal for achieving dimming control, some components of this high frequency signal are able to sneak through the data signal increasing noise and thus, affect the quality of the received signal. This then requires the introduction of a filtering circuit at the receiver to remove the added noise. The implemented PWM dimming technique is also able to provide a wide range of power levels for the implementation of Game Theory.

3.6 Experimental methodology and results

In order to validate the simulation results, the power allocation was implemented on the experimental setup and tested with different type of filters. The experimental setup uses optical filters that correspond to the values used for h_{rr}, h_{bb}, h_{rb} and h_{br} during simulations. In addition, the data rate across the blue and the red color subchannels was kept the same to ensure uniformity with the computer simulations as per (3.17). We are interested in the trends of the system's BER as a function of the power allocation, and therefore, for every power allocation in the red and blue subchannels, the corresponding BER was calculated. The same process was repeated with different type of filters to determine how the system behaves under different conditions and more importantly, how these optical filters affect the location of the optimal operating point. The experimental results are presented in Figure 3.13.

Figure 3.13 shows that the experimental results closely follow the same trends as predicted by the simulations. It is important to note the discrepancy between the simulated BER values and the experimental ones. This is due to the fact that in the computer simulations, the channel noise and attenuations were normalized. We can also see in Figure 3.13 that when a set of "good" optical filters (see Figure 3.2) which have minimal crosstalk is used on the red and blue colour subchannels, the optimal power allocation point lies closely within the $50 - 50\%$ mark. However,

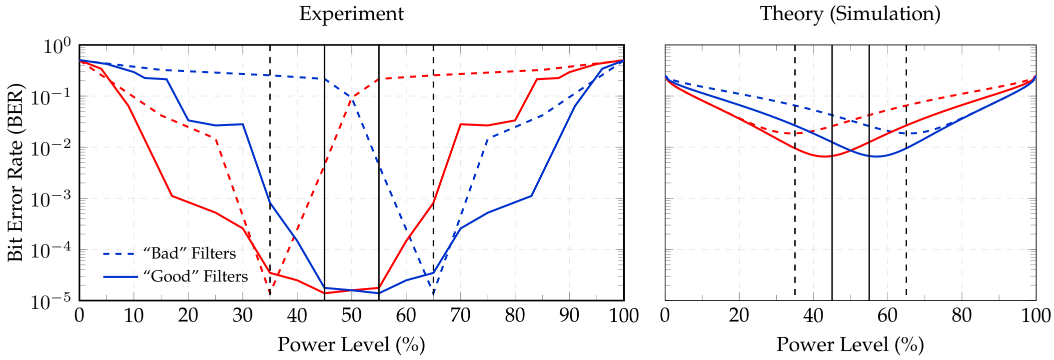

FIGURE 3.13: Simulations (right) and experimental (left) BER trends as a function of the power allocation in the red and blue subchannels for two different sets of filters. The experimental results closely follow the theoretical predictions in terms of the optimal power allocation. The vertical lines indicate the optimal power allocations based on the experimental results and the discrepancy to the theory is due to the granularity of the experiment.

it can be seen that when a "bad" filter such as the "turquoise" optical filter (see Figure 3.2) is used on the blue channel, the optimal power allocation point shifts significantly away from the half-way mark. In this case, a lot more power needs to be allocated to the blue subchannel to compensate for the frequency response of the "turquoise" filter. A similar pattern was observed with other type of red and blue filters. The optical "turquoise" filter use case scenario has been presented here to illustrate the impact that the filters' absorption coefficients have on the power allocation.

The objective of this work was to be able to predict the trends in the system's BER as a function of the power allocation in the red and blue colour subchannels, and to assess the impact that the optical filters used, have on the location of the optimal power allocation point. The results in Figure 3.13 show that the performance of WDM systems can be greatly improved by using a power allocation scheme that takes into consideration the frequency response of the optical filters used at the receiver.

Future work and improvement to the model should consider the possibility of predicting the exact BER values in addition to the trends and location of the optimal power point.

3.7 Summary

This chapter has shown that using an approach based on the water-filling algorithm, we are able to predict the trends in the overall performance of a WDM VLC system that employs red and blue LEDs. Experimental results show that the optimal power allocation point does not always lie close to the half-way mark, due to the fact that it is dependent on the type of optical filters used to discriminate between the wavelengths. This simplified model, although not yet able to predict the exact BER of the system, it can still adequately determine the optimal power levels in the different subchannels, which will result in the best overall performance for the multicarrier VLC system. The results obtained in this chapter can be extended to WDM VLC systems with three or any number of wavelengths. The model presented in this chapter can be used in the design and implementation of multicarrier VLC systems to minimize the crosstalk between subchannels. This will improve the performance and lead to efficient higher bandwidth in such systems.

Chapter 4

A Distributed Transmitter Power Control for multicarrier Visible Light Communication System based on the Refereed Game Theory

The next generation of networks will require cooperative behaviour between the different devices or entities that are connected to the network, and participate in the various interactive situations. However, cooperation between the interconnected entities is often hard to achieved due to the conflicting nature of their interests. The interaction between entities that make up the network is based on a set of rules, where each entity makes decisions that aim at maximizing its own selfish utility function. This is often at the expense of the overall system's performance and irrespective of the actions of neighbouring entities. Game Theory provides a theoretical framework that models strategic interactive situations between decision-making entities concerned about their own selfish benefit.

This chapter presents the results of a journal article which will be submitted to the IEEE Journal of Lightwave Technology. The reference to the paper is currently the following until submission and acceptance by the peer-review process: **Kamwangala C.**, Cox M., and Cheng L., "Distributed transmitter power control for a multicarrier visible light communication system", to be submitted to IEEE Journal of Lightwave Technology.

The main research idea was derived from a joint effort of **C. Kamwangala**, Prof. Ling Cheng and Mitchell Cox as a continuation of the work that was presented in Chapter 3. The software implementation used for data collection was coded in its entirety by **C. Kamwangala**. The same experimental setup hardware used in Chapter 3 was adopted for this part of the research work. The journal article is being written by **C. Kamwangala** under the supervision of Prof. Ling Cheng and Mitchel Cox to ensure that it meets the required quality standards for publication.

4.1 Game Theory in Communication Systems

The nature of cognitive radio systems makes them suitable for the application of Game Theory. This is due to the fact that cognitive radio networks comprise of various heterogeneous access technologies that coexist. Although these access networks often carry differing characteristics and capabilities, they are often required to cooperate in order to improve the overall network [68].

The interactions between the access networks in cognitive radios follow a trajectory that allows each network to achieve a selfish goal, irrespective of the actions of neighbouring network. Interactions between entities with conflicting goals is extensively studied in the broader field of Game Theory. Game Theory develops mathematical models and formulations that attempt to answer the question of how to achieve cooperative behaviour during interactions between self-managed entities, in order to achieve goals that are for the benefit of all participating entities in the network [68].

In Game Theory, a strategic interaction or game can be described as being in normal form or extensive form. A game is said to be in normal form when each player's strategies and the payoffs associated with each possible combination of choices can be fully listed. The extensive form of a game is when the rules of the game, the choices of strategies available to each player, the information available to a player and the payoffs each player receives are given [17, 68, 69]. When a game is played over multiple interactions such as in the case of the cognitive radio systems, it is said to be a repeated game. A single shot game is one that is played once such as the famous Prisoner's Dilemma game [17, 68].

A game can also be classified as either non-cooperative or cooperative. Non-cooperative games model situations where outcomes are completely decided by independent conflicting decision-makers without any external influence. In contrast, a cooperative game is a type of game where the outcome can be enforced by some third party contract or entity, usually known as the referee. The referee is responsible for enforcing the cooperation to ensure the optimal or equilibrium outcome is reached. Although the two are related, this project will focus on cooperative games.

A game in normal form consists of three main elements and can be expressed as G = {I,S,U}. The game consists of the following three elements:

- The set I = {1, . . . , n} of n players, i.e. the entities participating in the game.
- The set S = $S_1 \times . . . \times S_n$ of players' strategies, where Si contains the strategies available to the player i.
- The players' payoffs U = {u_1(.), . . . ,u_n(.)} which are functions indicating the values of different outcomes to the players.

A strategy $s_i \in$ S$_i$ is a choice that player *i* can perform.
The I-tuple **s** = (s_1, . . . ,s_n) is known as a strategy profile and uniquely defines an outcome, although the same outcome may be the result of different strategy profiles. More importantly, u_i(**s**) is the payoff that player *i* gets as a result of the outcome that results from using a specific strategy profile ***s*** [17].

Let us consider the transmit or remain quiet repeated network game involving two transmitters, player 1 and player 2 who need to transmit packets over a common channel to their respective receivers, R1 and R2 [70]. This multiple access network game is illustrated in Table 4.1. The two players have the following strategies

TABLE 4.1: Example payoff for the transmit or remain quiet repeated network game.

	P 2 Transmit	P 2 Quiet
P 1 Transmit	0,0	1,3
P 1 Quiet	3,1	0,0

available to them: each player can decide to transmit a packet or not transmit (remain quiet) represented by T and Q, respectively. If both players decide to transmit packets, it results in collision and loss of packets since this is a shared channel. The highest payoff for either player occurs when a player agrees to remain quiet while the other player is transmitting. This is known as the Nash's equilibrium point, named after John Nash's work on equilibrium point in strategic games [71,72]. Because this is a repeated game, players alternate between transmit or remain quiet in each round of the game.

In Game Theory, solving a game means determining the strategies for different players that ultimately lead to the Nash's equilibrium point. Nash's equilibrium describes a strategy profile wherein every entity or player participating in the game is playing a best response to the strategy choices of other players. When entities in a game play their best possible strategies, the game will reach Nash equilibrium.

Nash equilibrium in non-cooperative interactions is often hard to achieve as there is no incentive for the players to cooperative, given that they are only participating in the game for their own selfish interests. In such scenarios, cooperation between players can emerge when it is in their own best interest to do so and can lead to non-optimal outcome in certain situations. However, multiple signaling and communication between the entities participating in the game is often required to achieve equilibrium, which can create network overhead and more interference in the system [17,69,70].

The Refereed Game Theory is part of a family of cooperative games known as stochastic games. A stochastic game is one that is played in a sequential manner by participating entities wishing to achieve a certain common goal, based on the current state of the system as well as players' chosen actions. Each player chooses the best course of action or strategy based on information provided by the referee for the current state of the system. The Refereed Game Theory removes the need for communication between users and hence, reduces the amount of signaling and co-channel interference in the system as users get their information only from the referee. Furthermore, when well implemented the Refereed Game Theory can guarantee Nash equilibrium in a cooperative system.

Applications of Game Theory to analyze and resolve interactions between conflicting entities with selfish goals in cognitive radio networks have been reported in literature [15–17, 68, 73]. In this work, we attempt to use the tools of the Refereed Game Theory to analyze interactions between conflicting entities in a two-way visible light communication system.

4.2 A Distributed Power Control scheme for VLC Systems

Distributed power control is an optimization problem where individual entities make their own decisions in order to maximize their own utility function [17]. One of the interesting applications of visible light technology is in the field of home automation in smart homes, where there will be all kind of interconnected appliances that interact with each other through light. In such a scenario, the coordination between the different devices becomes a critical part in the implementation of the system to mitigate interference between the various entities in the network.

For the distributed scenario of the current project, although the different colour transmitters are part of the same transceiver circuit, each colour transmit power is controlled independently of the other colour transmitters. This is in contrast to the centralized case in Chapter 3 where the total available power was shared between the colour transmitters. This allows us to simulate a distributed VLC system where the colour transmitters would be located in different places like in the smart homes scenario, and study the effects that transmit power control can have on the overall performance of such systems.

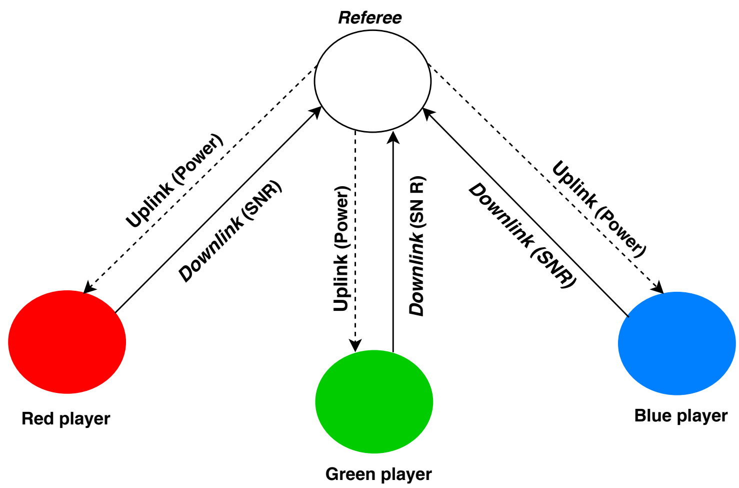

FIGURE 4.1: Illustration of the Refereed Game Scenario for a multicarrier RGB LED VLC system. Although the different colour transmitters are part of the same transceiver circuit, each colour transmit power is controlled independently of the other two colour. This is as opposed to the centralized case in Chapter 3 where the total power was shared between the colour transmitters. In the distributed scenario of the current project, the uplink feedback channel is used to enforce the punishment in the form of P_i^{uplink} on which each player relies to assess their received SNR by the referee. The downlink is still the forward channel from the transmitters to the receiver and is used for data transmission.

Consider a WDM RGB-LED VLC system as illustrated in Figure 4.1. As previously explained, the Refereed Game theory will be used in the current work to model the interaction of self-interested users in a multicarriers VLC channel. This theory deals with situations where outcomes can be enforced by some third party entity known as the referee. In our distributed VLC system, the uplink feedback channels from the receiver (the referee) to the individual colour transmitter will be used to enforce the outcome of the game through some form of punishment. In this project, the punishment is implemented in the form of P_i^{uplink} from the receiver to the transmitters, which each player relies on to assess their received SNR by the referee.

Before the Refereed Game can be implemented, it is crucial that the fundamental concepts of the theory be clearly defined and verified [17, 73]. This includes defining the players of the game, the actions available to the players, the objective to be achieved (the game), the referee and the punishment. The rest of this section will be dedicated to defining the building blocks of the Refereed Game for our VLC system.

4.2.1 The Players

Each individual colour subchannel represents an entity in the network and participate in the game. These entities which are often referred to as players must cooperate and obey the rules of the game in order to achieve a better overall system's performance. In the Refereed Game Theory, the rules of the game can be enforced through the referee who is responsible for punishing entities who do not play by the rules.

4.2.2 The Game

As opposed to the centralized scenario in Chapter 3 where the constraint was applied to the total available power at transmitter shared between the different colour transmitters, in the distributed implementation, the constraint on the optimization is applied to the power P_i^{uplink} in the uplink channel. This is the power used by the referee to enforce the rules of the game given that the different players in the game rely on this power for information about the quality of their individual transmission.

Suppose that the referee has power P_{ref} available for the uplink broadcast to the different colour channels. The objective (the game) is to maximize the channel capacity and can be formulated as follows

$$\text{maximize} \quad \sum_{i=1}^{3} \log_2 (1 + SNR_i) \tag{4.1}$$

subject to

$$\sum_{i=1}^{3} P_i^{uplink} \quad \leq \quad P_{ref} \tag{4.2}$$

Where P_i^{uplink} represents the individual uplink power from the central agent to the different colour channels. SNR_i is the received signal-to-noise ratio of a player at the receiver.

Consider an infinitely repeated version of the above game where a player is faced with the challenge of deciding which action to take. The rules of the game are such that the system seek to optimize the overall system BER and uses the water-filling algorithm as described in Chapter 3 to determine the optimal power levels for each colour transmitter. A player can either increase or decrease his transmit power and each of these actions has a reward associated with it in the form of P_i^{uplink} in the uplink channel. If the payoff associated with each action is constant, all a player needs in order to maximize his payoff forever is to do a linear search for an action that derives the best benefits. However, if the payoff associated with each action varies across iterations of the game, that is, the same action can result in a gain or a loss, then a learning algorithm is required to assist the decision of the player.

4.2.3 The Referee

Once the optimal operating point for the system has been determined, the referee notifies the respective players of the appropriate power levels and the system must penalize any colour carrier whose received power is higher than the chosen threshold. This could be accomplished by decreasing the performance on the feedback channel for the particular colour subchannel who acts in a greedy manner. However, it is important that the punishment be not too harsh so as to make the players deviate from the optimal point with the game unable to converge.

4.2.4 The Punishment

In the current project, the feedback channel was implemented in software as a way to simulate a two-way system on the experimental setup. Because the system is a two-way communication system, the independent colour channels all rely on the feedback from the central agent and thus, the punishment can be enforced through the feedback channel. The SNR of each colour subchannel is affected by the crosstalk interference from the other two colour subchannels, which in turn is a function of the allocated power in those two channels. The SNR can be expressed as follows

$$SNR_R = \frac{|h_{rr}|^2 P_R}{N_o + \Gamma_R}, \quad SNR_G = \frac{|h_{gg}|^2 P_G}{N_o + \Gamma_G} \quad \text{and} \quad SNR_B = \frac{|h_{bb}|^2 P_B}{N_o + \Gamma_B} \tag{4.3}$$

where P_i is the power of the respective LED, N_o is the normalized shot and background noise in the system, and Γ_i is the total interference from the other channels, given by

$$\begin{aligned} \Gamma_R &= |h_{rg}|^2 P_G + |h_{rb}|^2 P_B \\ \Gamma_G &= |h_{gr}|^2 P_R + |h_{gb}|^2 P_B \\ \Gamma_B &= |h_{br}|^2 P_R + |h_{bg}|^2 P_G. \end{aligned} \tag{4.4}$$

Therefore, if the system seeks a received power that optimizes the overall system BER, colour transmitters in the network must cooperate and work together while abiding by the rules of the game. In order to ensure that the rules of the game are respected, the referee should punish any entity whose received power is above the prescribed threshold. This could be accomplished by deliberately decreasing the uplink power of the culprit in the feedback channel which the players use to assess the quality of their transmissions. From the players' perspective, a higher uplink power means that the receiver is accepting their packets, whilst a lower uplink power means their packets are being dropped. In addition, because the power in the uplink channel is bounded by P_{ref}, maximum power means that the player should not continue to increase his power level.

An example of a punishment can be formulated by ensuring that the uplink power P_i^{uplink} of each player in the feedback channel is a function of the difference between the player's received signal-to-noise ratio level SNR_i, and the predetermined optimal level SNR_i^*. This can be expressed in mathematical form as follows

$$P_i^{uplink} = f(SNR_i - SNR_i^*)$$
$$\therefore SNR_i = f^{-1}(P_i^{uplink}) + SNR_i^* \tag{4.5}$$

From (4.5), we notice that the uplink power P_i^{uplink} and the player's received signal-to-noise ratio level SNR_i are inverse functions of each other. This requires that the following restrictions be placed on possible candidate functions used to formulate the punishment.

- $0 \leq f(SNR_i - SNR_i^*) \leq P_{ref}$ for all values of $(SNR_i - SNR_i^*)$ and
- $f(0) = P_{i(max)}^{uplink}$

The first restriction ensures that the power P_i^{uplink} in the uplink channel is bounded and subjects to the referee's available P_{ref}. In addition, maximum uplink $P_{i(max)^{uplink}}$ power ensures that a player whose received SNR is equal to the predetermined optimal level, stops increasing his power for convergence of the game. Given that the referee's uplink power P_i^{uplink} and the player's received signal-to-noise ratio level SNR_i are inverse functions of each other, the original problem can now be rewritten as

$$\text{maximize} \quad \sum_{i=1}^{3} \log_2 \left(1 + f^{-1}(P_i^{uplink}) + SNR_i^*\right) \tag{4.6}$$

subject to

$$\sum_{i=1}^{3} P_i^{uplink} \quad \leq \quad P_{ref} \tag{4.7}$$

Various type of functions can be used to generate the punishment, each with different levels of severity. Figure 4.2 below, shows the different profiles for the punishment function. The x-axis represents the gap between the optimal signal-to-noise ratio SNR_i^* and a player's received signal-to-noise ratio SNR_i. The zero point on the x-axis indicates that the player is operating at the optimal point and corresponds to the maximum uplink power on the y-axis.

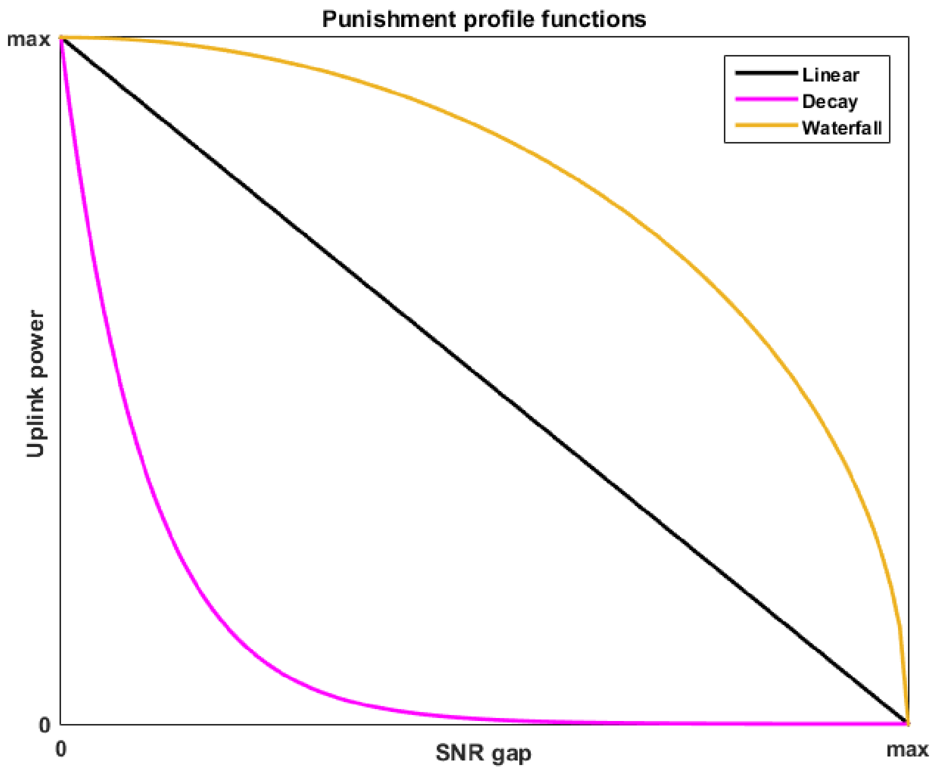

FIGURE 4.2: Possible punishment profile functions.

A punishment is considered harsh if smaller deviations from the set optimal operating point result in much larger penalties. Similarly, a punishment curve is considered lenient if smaller deviations from the optimal point also result in smaller penalties. The linear profile illustrated in Figure 4.2 allows for a constant rate of change in the punishment imposed on a greedy player, whilst in the exponential decay profile, very small deviations from the pre-determined optimal operating point can results in a bigger punishment. For the waterfall profile shown in Figure 4.2, large deviations from the pre-determined operating point often only result in a smaller punishment as compared to the exponential profile in Figure 4.2.

In the absence of a punishment in the payoff function and a referee to enforce this punishment, players choose a course of actions that maximize their own utility function for their selfish interests. However, if the payoff associated with each action varies across iterations of the game and the prospect of being punished for players who do not obey the rules of the game, the Refereed Game Theory can act as a no-regret algorithm.

The concept of no-regret is based on the notion that no player can do strictly better by deviating from the best response strategy, given that the other players are also bound by the same rules. The next section discusses the implementation of the no-regret decision making algorithm in the current distributed VLC system.

4.3 No-Regret Learning Algorithm

Several decision making algorithms based on statistical learning theory for cooperative interactions between participating entities with conflicting interests, in distributed networks have been developed and are documented in literature [74, 75].

Algorithm 1 No-regret learning algorithm

1 . Initialization: Players start from a reference point and select an arbitrary course of action.

2 . System performs a dry run and referee determines optimal operating point for each players using the water-filling algorithm.

3 . Players are notified of their respective target operating points through the feedback channel.

4 . After each iteration of the game, players are given reward by the referee in terms of power in the feedback channel.

5 . Players use the reward information from the referee to adjust their transmit power with respect to the optimal operating points, in order to get an even better uplink power.

6 . Confirmation: Check that each player's course of action is converging towards the equilibrium point. If not, go back to step 1, otherwise maintain current equilibrium until channel conditions change, and the referee decides to update optimal operating point targets.

In this project, we implemented a version of the well-known no-regret algorithm using state machines approach. The no-regret algorithm is a statistical learning algorithm that uses previous choices from past interactions between participating players or entities in the game to determine rewards in current choices, and predict choices that will be made in future interactions. The algorithm is structured in such a way that the payoff obtained from using the algorithm is always greater than the payoff that can be gained from using alternative strategies [69].

A flow chart diagram of the implemented no-regret learning algorithm is shown in Figure 4.3 below.

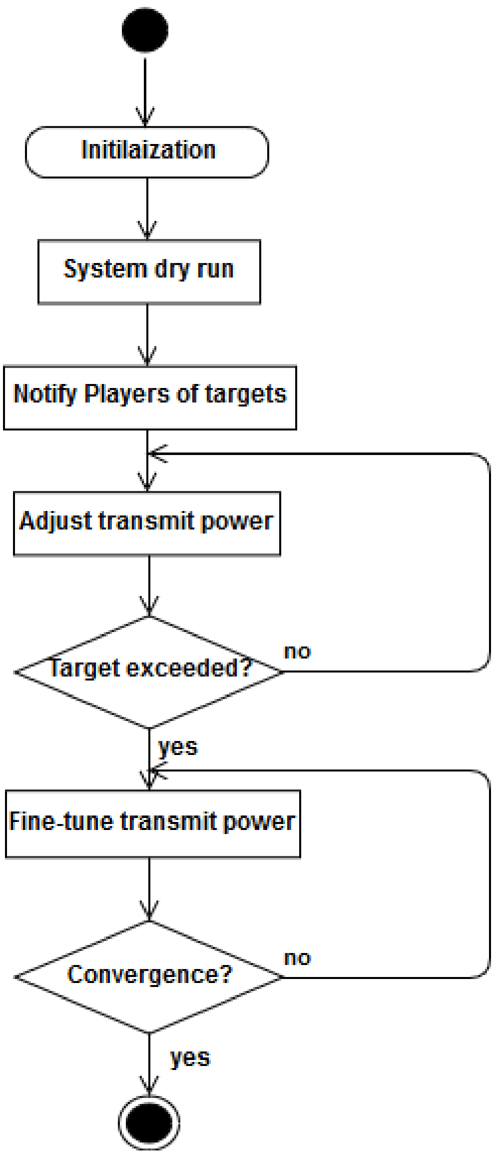

FIGURE 4.3: Flow chart of the implemented no-regret algorithm.

In this work, convergence is defined as the equilibrium point where all colour transmitters are operating at their respective pre-set optimal operating points and no power increase or decrease take place in the system.

4.4 Results and Discussions

In this section, we take a look at the experimental results for the linear and the waterfall profiles which have been implemented for the current research project. The linear punishment profile can be expressed in mathematical form as follows

$$y = -mx + c \tag{4.8}$$

The constant c represents the referee's maximum power that can be allocated to the uplink channel for a specific player and thus, cannot be changed. The gradient m dictates how harsh the punishment is and how aggressive the players will be when trying to abide by the rules of the game. In this work, the same punishment profile is always implemented for both players. However, the pre-determine optimal operating point for each player is based on the output of the water-filling algorithm and depends on the characteristics of the optical filters used in our experimental setup (see Figure 3.2).

In the first scenario illustrated by Figure 4.4, slow gradient linear punishment functions are chosen for the players strategies. It can be seen that the two players (red and blue channel carriers) move towards their respective target equilibrium points in a very smooth manner due to the lenient nature of the punishment.

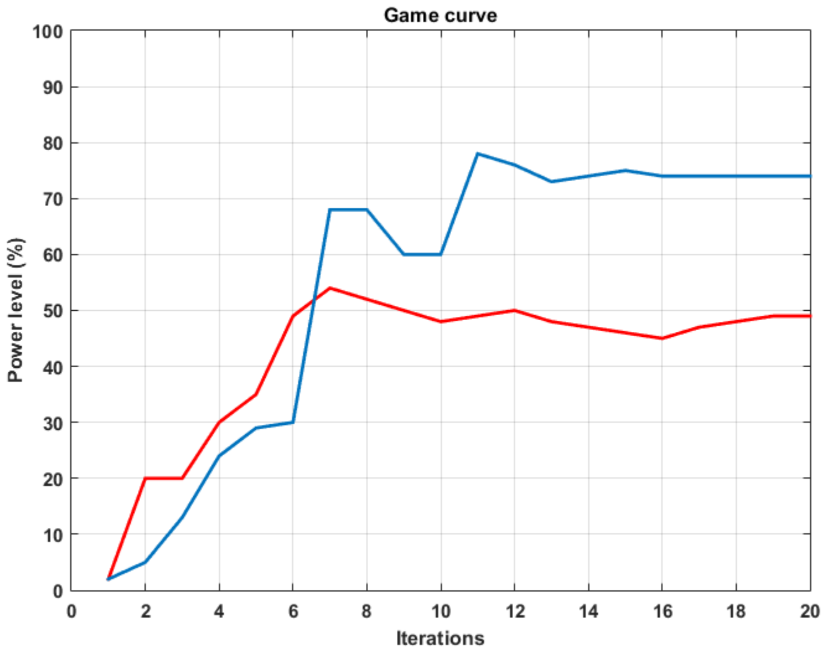

FIGURE 4.4: Game curve for the red and blue sub-channels: slow gradient and farther starting point.

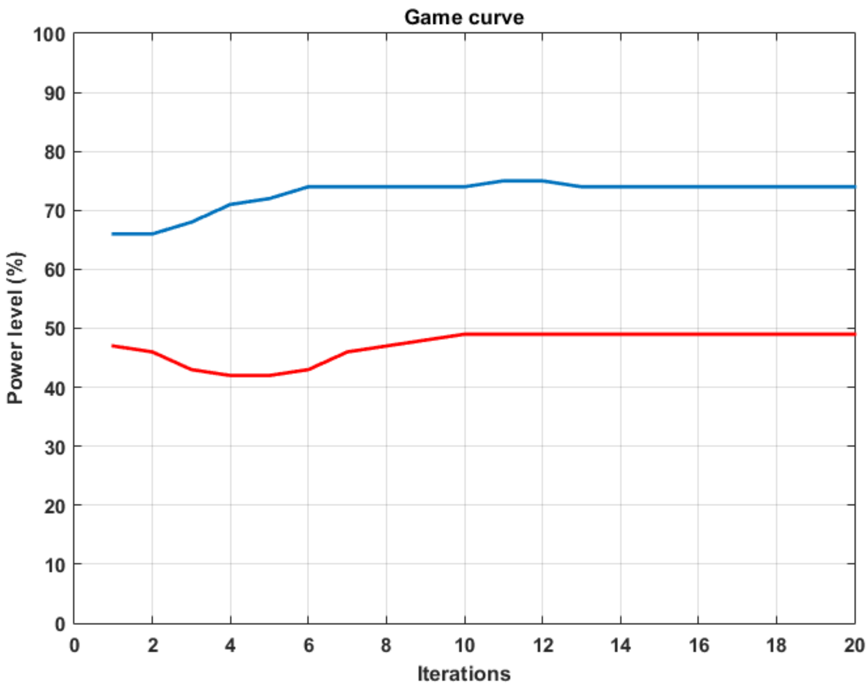

FIGURE 4.5: Game curve for the red and blue sub-channels: slow gradient and closer starting point.

In Figure 4.5 above, the starting points for the two players are chosen relatively closer to the equilibrium points, which lead to a faster convergence of the game.

For the second scenario in Figure 4.6, a steeper gradient is chosen for the profile functions, which means a much harsher punishment for the players. This results in a very aggressive mode as the players struggle to adjust their respective transmit powers to get to the equilibrium state. Furthermore, it can be seen that after 20 iterations, the red player has not yet reached equilibrium. The red player's power level constantly fluctuates around the operating point.

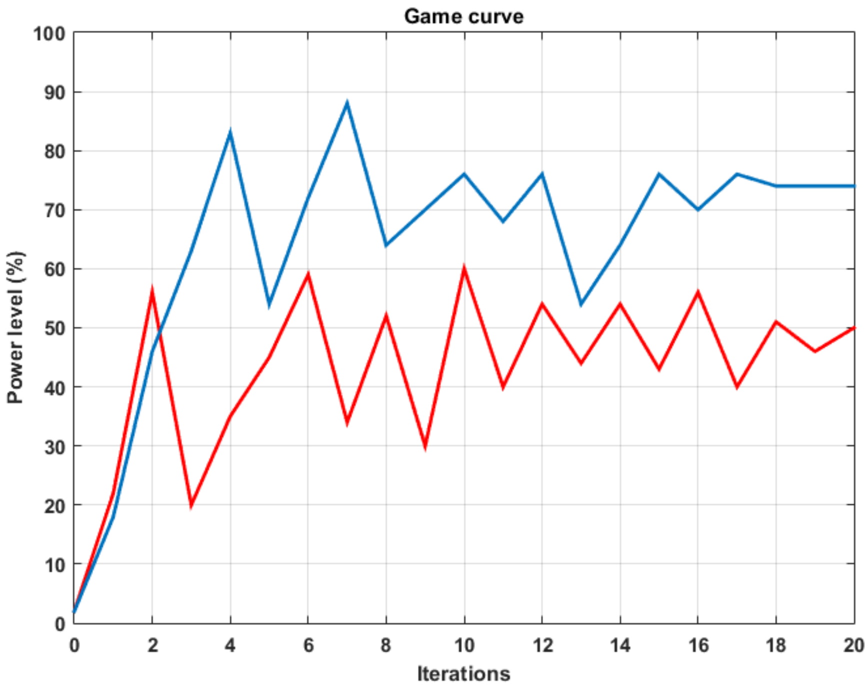

FIGURE 4.6: Game curve for the red and blue sub-channels: fast gradient and farther starting point.

Choosing starting points that are closer to the optimal points for the players as in Figure 4.7, lead to smaller fluctuations around the operating points and sometimes the game converges.

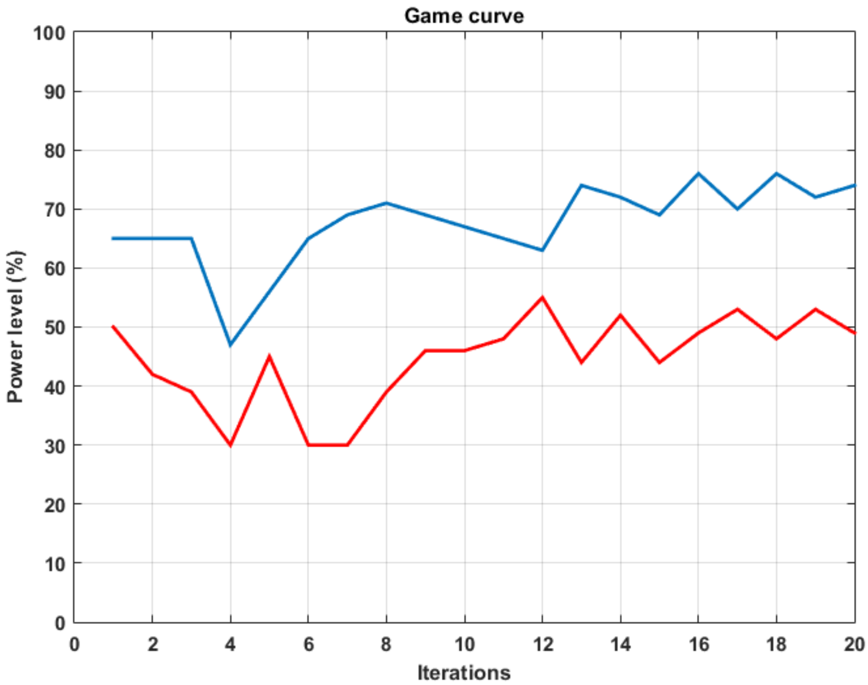

FIGURE 4.7: Game curve for the red and blue sub-channels: fast gradient and closer starting point.

The results in Figure 4.8 shows the game curve for the waterfall punishment profile. One interesting observation is the fact that with this profile players are able to deviate from the optimal point within a certain range because the punishment is not too harsh.

Ideally, harsher punishments should lead to faster convergence of the game. However, in some cases if the punishment is extremely harsh, it would result in a lot of fluctuations and, in some cases prevents the convergence of the game. In the case of more lenient punishments, the game should take longer to converge because players are afforded more freedom and tend to settle at a higher point then the pre-determine operating point.

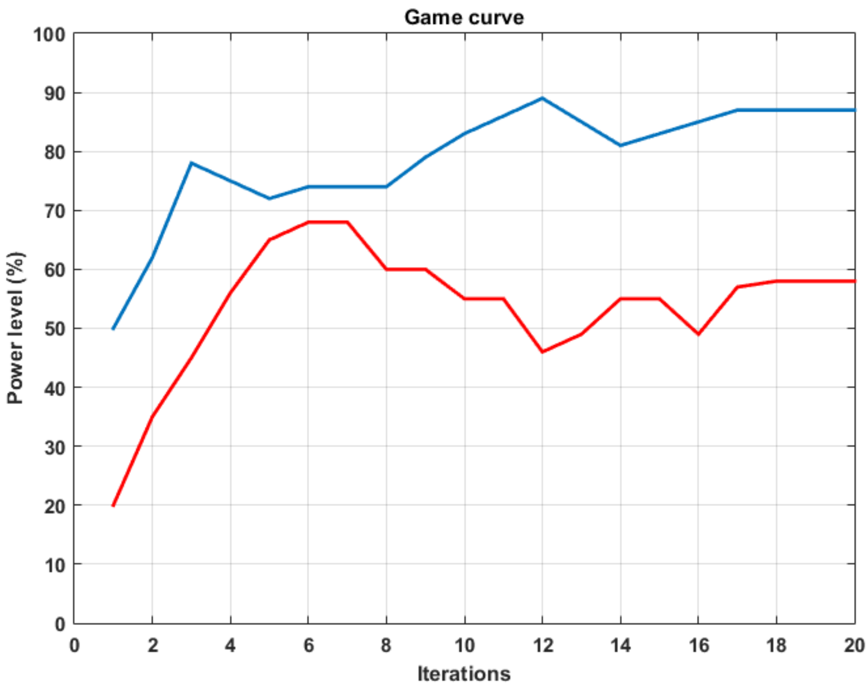

FIGURE 4.8: Game curve for the red and blue sub-channels: waterfall profile.

4.5 Future work

Future work should consider the possibility of predicting the required number of iterations for convergence, as well as having different punishment profile in the same game depending on the players' behaviour. In addition, the results in Figure 4.4 and Figure 4.6 show that when players initially start at the same reference point, the power level for the red LED increases much faster than that of the blue LED even though they have the same punishment profile function. This is due to the difference in the optical output power of the LEDs used.

4.6 Summary

This chapter has shown that the Refereed Game Theory can be used to enforce a pre-determined optimal operating point in a distributed transmitter power control scenario for an RGB-based visible light communication system. Two different scenarios were explored using the linear profile punishment and the waterfall profile. in the first case, with a more lenient punishment profile characterized by a slow gradient, results show that players move towards the equilibrium in a smooth approach. In the second scenario however, for a harsher punishment linear profile characterized by a steep gradient, players make decisions in a very aggressive manner, which can often lead to a non-convergence of the game in some cases. However, in both cases, it can be seen that when the outcome is enforced by a third party entity, cooperation between the players can be achieved.

Chapter 5

Conclusion

The reason d'être of this research work is the question "*What are the effects of optimal transmitter power control on the performance of an indoor, WDM-OOK modulated, RGB-based multicarrier VLC system, in terms of overall system BER?*". Chapter 2 presents the state of research in the VLC technology, the basic building blocks of VLC systems, and the different multicarrier modulation schemes that are currently used. A literature review on the use of coordinated interference management in VLC systems is also discussed to provide the reasoning behind the choices made for this research. In Chapter 3, the results of the special issue article published in Wiley's Transactions on Emerging Telecommunications Technologies, which demonstrate the use of centralized transmitter power control to predict the trends in the BER performance of a multicarrier VLC system that employs red and blue LEDs are presented. Although not able to predict the exact BER of the system, the developed centralized transmitter power control scheme can still adequately determine the optimal power levels in the red and blue subchannels that will result in the best overall performance for the multicarrier VLC system. Thereafter, Chapter 4 puts forward the formulation and implementation of a distributed transmitter power control scheme based on the Refereed Game Theory. It was shown that for lenient punishment profiles characterized by a slow gradient, players move toward the equilibrium optimal operating point in a smooth approach. However, for a harsher punishment profile characterized by a steep gradient, players make decisions in a very aggressive manner, which can often lead to a non-convergence of the game in some cases. That being said, in both cases, it can be seen that when the outcome is enforced by a third party entity, cooperation between the players can be achieved. Results from this chapter are to be submitted to IEEE Journal of Lightwave Technology. From the results presented in Chapter 3 and Chapter 4, it can be concluded that the performance of multicarrier WDM VLC systems can be improved using transmitter power control. The research objectives defined in Chapter 1 have thus been accomplished, and the research question has been answered.

5.1 Recommendations for Future Work

As discussed in Chapter 3, the developed centralized transmitter power control scheme only gives the location of the optimal operating power point and predicts the trends in the BER performance. Future work and improvement to the model should consider the possibility of predicting the exact BER values, in addition to the trends and location of the optimal power point. Additionally, for the distributed power control scheme, it would be interesting to be able to determine the required number of iterations for the converge of the game, as well as having different punishment profiles in the same game for the players, and doing a performance comparison for these scenarios. Furthermore, the results obtained in this research work should be extended and tested not only on systems which use red, green and blue LEDs but also on those that use any number of wavelengths. Finally, it would be interesting to do a full set of performance benchmarks between a system with the developed transmitter power control and one without it.

As seen in the literature review in Chapter 2, there is little existing research on the use of Game Theory to solve problems associated with cooperative interactions in VLC systems. IoT and 5G networks will require cooperative behaviour between the different devices connected to the network. Due to the fact that VLC is seen as a potential enabler for this technology, it becomes important for more research to be done in using tools such as Game Theory to investigate cooperative interactions in VLC systems as a way to mitigate crosstalk interference in WDM systems.

5.2 Summary

In Chapter 1, the current research work aimed to answer the question "*What are the effects of optimal transmitter power control on the performance of an indoor, WDM-OOK modulated, RGB-based multicarrier VLC system, in terms of overall system BER?*". Results presented both in Chapter 3 and Chapter 4 show that optimal transmitter power control can be used to improve the performance of WDM VLC system by reducing the crosstalk interference which often affects these systems. This is especially important in situations where the optical colour filters used at the receiver to discriminated between the incoming colour signals have a wideband frequency response. Recommendations for possible future work to improve on the current project were made and a conclusion has been drawn.

References

[1] P. H. Pathak, X. Feng, P. Hu, and P. Mohapatra, "Visible Light Communication, Networking, and Sensing: A Survey, Potential and Challenges," *IEEE Communications Surveys Tutorials*, vol. 17, no. 4, pp. 2047–2077, 2015.

[2] D. C. O'Brien, "Visible Light Communications: Challenges and potential," *IEEE Photonic Society 24th Annual Meeting, PHO 2011*, vol. 3, pp. 365–366, 2011.

[3] Y. Tanaka, T. Komine, S. Haruyama, and M. Nakagawa, "Indoor visible communication utilizing plural white LEDs as lighting," *Personal, Indoor and Mobile Radio Communications, 2001 12th IEEE International Symposium on*, vol. 2, pp. F–81,F–85, Oct. 2001.

[4] S. H. Chen and C. W. Chow, "Color-Shift Keying and Code-Division Multiple-Access Transmission for RGB-LED Visible Light Communications Using Mobile Phone Camera," *IEEE Photonics Journal*, vol. 6, no. 6, pp. 1–6, Dec 2014.

[5] C. Danakis, M. Afgani, G. Povey, I. Underwood, and H. Haas, "Using a CMOS camera sensor for visible light communication," *2012 IEEE Globecom Workshops*, pp. 1244–1248, Dec 2012.

[6] D. Tsonev, H. Chun, S. Rajbhandari, J. McKendry, S. Videv, E. Gu, M. Haji, S. Watson, A. Kelly, G. Faulkner, M. Dawson, H. Haas, and D. O'Brien, "A 3-Gb/s Single-LED OFDM-Based Wireless VLC Link Using a Gallium Nitride uLED," *Photonics Technology Letters, IEEE*, vol. 26, no. 7, pp. 637–640, Apr. 2014.

[7] S. Dimitrov and H. Haas, “Principles of LED Light Communications: Towards Networked Li-Fi,” *Cambridge University Press*, pp. 253–256, 2015.

[8] M. Uysal, C. Capsoni, Z. Ghassemlooy, A. Boucouvalas, and E. Udvary, Eds., *Optical Wireless Communications*, ser. Signals and Communication Technology. Springer International Publishing, 2016.

[9] M. Z. Afgani, H. Haas, H. Elgala, and D. Knipp, “Visible Light Communication Using OFDM,” *2nd International Conference on Testbeds and Research Infrastructures for the Development of Networks and Communities, 2006. TRIDENTCOM 2006*, pp. 129–134, 2006.

[10] J. Vučić, C. Kottke, S. Nerreter, K. D. Langer, and J. W. Walewski, “513 Mbit/s Visible Light Communications Link Based on DMT-Modulation of a White LED,” *Journal of Lightwave Technology*, vol. 28, no. 24, p. 3512–3518, Dec 2010.

[11] W. Yu and J. M. Cioffi, “On constant power water-filling,” *ICC 2001. IEEE International Conference on Communications. Conference Record (Cat. No.01CH37240)*, vol. 6, no. 4, pp. 1665–1669, 2001.

[12] Q. Qi and Y. L. Yang, “An Efficient Water-Filling Algorithm for Power Allocation in OFDM-Based Cognitive Radio Systems,” *CSE Conference and Workshop Papers*, 2012.

[13] J. Wu, L. Yang, and X. Liu, “Resource allocation based on linear waterfilling algorithm in CR systems,” *7th International Conference on Wireless Communications, Networking and Mobile Computing, WiCOM 2011*, no. 1, pp. 26–29, 2011.

[14] W. J. Shin and D. I. Kim, “Penalized iterative waterfilling algorithm for multi-cell and multi-user OFDMA systems,” *IEEE International Symposium on Personal, Indoor and Mobile Radio Communications, PIMRC*, pp. 2245–2249, 2009.

[15] J. Wu, "A Survey of Game Theory in Wireless Networking Design," *Computer Engineering*, no. 995848098, pp. 1–7.

[16] a.B. MacKenzie and S. Wicker, "Game theory in communications: motivation, explanation, and application to power control," *GLOBECOM'01. IEEE Global Telecommunications Conference (Cat. No.01CH37270)*, vol. 2, pp. 821–826, 2001.

[17] V. Gajic, "Game Theory in Communications: A Study of Two Scenarios," PhD Dissertation, École Polytechnique Fédérale de Lausanne, 2010.

[18] J. Zander, "Performance of optimum transmitter power control in cellular radio systems," *IEEE Transactions on Vehicular Technology*, vol. 41, no. 1, pp. 57–62, 1992.

[19] C. Kamwangala, M. Cox, and L. Cheng, "Transmitter power control for a multicarrier visible light communication system," *Trans Emerging Tel Tech.*, 2018; e3453. https://doi.org/10.1002/ett.3453.

[20] H. Elgala, R. Mesleh, and H. Haas, "Indoor optical wireless communication: potential and state-of-the-art," *IEEE Commun. Mag*, vol. 49, no. 9, Sept 2011.

[21] H. Haas, "Wireless Data from Every Light Bulb," *TEDGlobal*, Aug 2011, Accessed: 2018-09-30. [Online]. Available: http://bit.ly/tedvlc

[22] M. Wall, "'Li-Fi' via LED Light Bulb Data Speed Breakthrough," Oct 2013, Accessed: 2018-03-24. [Online]. Available: http://www.bbc.co.uk/news/technology-24711935

[23] J. C. Lin, "Cancer Occurrences in Laboratory Rats From Exposure to RF and Microwave Radiation," *IEEE Journal of Electromagnetics, RF and Microwaves in Medicine and Biology*, vol. 1, no. 1, pp. 2–13, Jun 2017.

[24] J. Lin, "Microwave Signal at the U.S. Embassy in Moscow [Health Matters]," *IEEE Microwave Magazine*, vol. 19, no. 2, pp. 20–22, Mar 2018.

[25] N. L. A. Azhar, R. Ariffin, H. Abdullah, and M. Omar, "A pregnant women vest and window curtain as an RF electromagnetic shielding," *2014 IEEE Symposium on Industrial Electronics Applications (ISIEA)*, pp. 71–75, Sept 2014.

[26] J. Higashiyama and Y. Tarusawa, "RF exposure compliance assessment for radio base station with built-in antenna," *10th International Symposium on Electromagnetic Compatibility*, pp. 90–93, Sept 2011.

[27] S. Hranilovic, *Wireless Optical Communication Systems*, ser. Signals and Communication Technology. Springer-Verlag New York, 2005, eBook ISBN 978-0-387-22785-6.

[28] C.-H. Yeh, Y.-L. Liu, and C.-W. Chow, "Real-time white-light phosphor-LED visible light communication (VLC) with compact size." *Optics express*, vol. 21, no. 22, 2013.

[29] J. Vučić, C. Kottke, S. Nerreter, K. Habel, A. Buttner, K. D. Langer, and J. W. Walewski, "125 Mbit/s over 5 m wireless distance by use of OOK-Modulated phosphorescent white LEDs," *2009 35th European Conference on Optical Communication*, vol. 2, pp. 1–2, Sept 2009.

[30] H. L. Minh, D. O'Brien, G. Faulkner, L. Zeng, K. Lee, D. Jung, and Y. Oh, "High-speed visible light communications using multiple-resonant equalization," *IEEE Photon. Technol. Lett*, vol. 20, no. 14, pp. 1243–1245, Jul 2008.

[31] Y. Wang, X. Huang, L. Tao, J. Shi, and N. Chi, "45-Gb/s RGB-LED based WDM visible light communication system employing CAP modulation and RLS based adaptive equalization," *Optics Express*, vol. 23, no. 10, p. 13626, 2015.

[32] N. Chi, M. Zhang, Y. Zhou, and J. Zhao, "3.375-Gb/s RGB-LED based WDM visible light communication system employing PAM-8 modulation with phase

shifted Manchester coding," *Optics Express*, vol. 24, no. 19, pp. 21 663–21 673, 2016.

[33] C. Kottke, J. Hilt, K. Habel, J. Vučić, and K. Langer, "1.25 Gbit/s visible light WDM link based on DMT modulation of a single RGB LED luminary," *Optical Communications (ECOC), 2012 38th European Conference and Exhibition on*, pp. 1–3, Sept 2012.

[34] A. R. Ndjiongue, H. Ferreira, and T. Ngatched, "Visible Light Communications (VLC) Technology," *Wiley Encyclopedia of Electrical and Electronics Engineering*, pp. 1–15, Jun 2015.

[35] W. O. Popoola, Z. Ghassemlooy, J. I. H. Allen, E. Leitgeb, and S. Gao, "Free-space optical communication employing subcarrier modulation and spatial diversity in atmospheric turbulence channel," *IET Optoelectronics*, vol. 2, no. 1, pp. 16–23, Feb 2008.

[36] S. Kaur, W. Liu, and D. Castor, "VLC dimming support IEEE 802.15-09-0641-00-0007." [Online]. Available: https://mentor.ieee.org/802.15/dcn/09/15-09-0641-00-0007-vlc-dimming-proposal.pdf

[37] J. K. Kwon, "Inverse source coding for dimming in visible light communications using NRZ-OOK on reliable links," *IEEE Photon. Technol. Lett*, vol. 22, no. 19, pp. 1455–1457, Oct 2010.

[38] Y. Zhao and J. Vongkulbhisal, "Design of Visible Light Communication Receiver for On-Off Keying Modulation by Adaptive Minimum-Voltage Cancelation," *Engineering Journal*, vol. 17, no. 4, pp. 637–640, Oct 2013.

[39] S. Muthu and J. Gaines, "Red, green and blue LED-based white light source: implementation challenges and control design," in *38th IAS Annual Meeting on Conference Record of the Industry Applications Conference, 2003.*, vol. 1, Oct 2003, pp. 515–522.

[40] G. Ntogari, T. Kamalakis, J. Walewski, and T. Sphicopoulos, "Combining illumination dimming based on pulse-width modulation with visible light communications based on discrete multitone," *IEEE/OSA Journal of Optical Communications and Networking*, vol. 3, no. 1, pp. 56–65, Jan 2011.

[41] H. Sugiyama, S. Haruyama, and M. Nakagawa, "Brightness Control Methods for Illumination and Visible-Light Communication Systems," in *2007 Third International Conference on Wireless and Mobile Communications (ICWMC'07)*, Mar 2007, pp. 78–78.

[42] M. Arun, *Advanced Free Space Optics (FSO): A Systems Approach*, ser. Signals and Communication Technology. Springer-Verlag New York, 2015, vol. 186.

[43] S. C. J. Lee, S. Randel, F. Breyer, and A. M. J. Koonen, "PAM-DMT for Intensity-Modulated and Direct-Detection Optical Communication Systems," *IEEE Photonics Technology Letters*, vol. 21, no. 23, pp. 1749–1751, Dec 2009.

[44] Q. Lu, X. Ji, and K. Huang, "Clipping distortion analysis and optimal power allocation for ACO-OFDM based visible light communication," in *2014 4th IEEE International Conference on Information Science and Technology*, Apr 2014, pp. 320–323.

[45] N. Fernando, Y. Hong, and E. Viterbo, "Flip-OFDM for optical wireless communications," in *2011 IEEE Information Theory Workshop*, Oct 2011, pp. 5–9.

[46] M. Biagi, A. M. Vegni, and T. D. C. Little, "LAT indoor MIMO-VLC – Localize, access and transmit," in *2012 International Workshop on Optical Wireless Communications (IWOW)*, Oct 2012, pp. 1–3.

[47] W.-Y. Lin, C.-Y. Chen, H.-H. Lu, C.-H. Chang, Y.-P. Lin, H.-C. Lin, and H.-W. Wu, "10m/500Mbps WDM visible light communication systems," *Opt. Express*, vol. 20, no. 9, pp. 9919–9924, Apr 2012. [Online]. Available: http://www.opticsexpress.org/abstract.cfm?URI=oe-20-9-9919

[48] F. M. Wu, C. T. Lin, C. C. Wei, C. W. Chen, Z. Y. Chen, H. T. Huang, and S. Chi, "Performance Comparison of OFDM Signal and CAP Signal Over High Capacity RGB-LED-Based WDM Visible Light Communication," *IEEE Photonics Journal*, vol. 5, no. 4, pp. 7 901 507–7 901 507, Aug 2013.

[49] J. Vučić, C. Kottke, K. Habel, and K. Langer, "803 Mbit/s visible light WDM link based on DMT modulation of a single RGB LED luminary," in *2011 Optical Fiber Communication Conference and Exposition and the National Fiber Optic Engineers Conference*, Mar 2011, pp. 1–3.

[50] Y. Wang, X. Huang, L. Tao, and N. Chi, "1.8-Gb/s WDM visible light communication over 50-meter outdoor free space transmission employing CAP modulation and receiver diversity technology," in *2015 Optical Fiber Communications Conference and Exhibition (OFC)*, Mar 2015, pp. 1–3.

[51] C. Kamwangala, "Performance comparison between single-carrier and multicarrier modulation schemes for visible light communication," *Tech Laboratory project report, School of Electrical and Information Engineering, Wits University*, pp. 1–5, 2016.

[52] S. Chen and C. Chow, "Color-filter-free WDM MIMO RGB-LED visible light communication system using mobile-phone camera," in *2014 13th International Conference on Optical Communications and Networks (ICOCN)*, Nov 2014, pp. 1–4.

[53] D. G. Lowe, "Distinctive image features from scale-invariant keypoints," *International journal of computer vision*, vol. 60, no. 2, pp. 91–110, Nov 2004. [Online]. Available: https://doi.org/10.1023/B:VISI.0000029664.99615.94

[54] D. Bykhovsky and S. Arnon, "Multiple Access Resource Allocation in Visible Light Communication Systems," *Journal of Lightwave Technology*, vol. 32, no. 8, pp. 1594–1600, Apr 2014.

[55] M. B. Rahaim, A. M. Vegni, and T. D. C. Little, "A hybrid Radio Frequency and broadcast Visible Light Communication system," in *2011 IEEE GLOBECOM Workshops (GC Wkshps)*, Dec 2011, pp. 792–796.

[56] Z. Yu, R. J. Baxley, and G. T. Zhou, "Multi-user MISO broadcasting for indoor visible light communication," in *2013 IEEE International Conference on Acoustics, Speech and Signal Processing*, May 2013, pp. 4849–4853.

[57] M. Kashef, M. Abdallah, K. Qaraqe, H. Haas, and M. Uysal, "Coordinated interference management for visible light communication systems," *IEEE/OSA Journal of Optical Communications and Networking*, vol. 7, no. 11, pp. 1098–1108, Nov 2015.

[58] Y. Wang, Y. Shao, H. Shang, X. Lu, Y. Wang, J. Yu, and N. Chi, "875-Mb/s asynchronous bi-directional 64QAM-OFDM SCM-WDM transmission over RGB-LED-based visible light communication system," in *2013 Optical Fiber Communication Conference and Exposition and the National Fiber Optic Engineers Conference (OFC/NFOEC)*, Mar 2013, pp. 1–3.

[59] T. Cogalan, H. Haas, and E. Panayirci, "Power Control-Based Multi-User Li-Fi Using a Compound Eye Transmitter," in *2015 IEEE Global Communications Conference (GLOBECOM)*, Dec 2015, pp. 1–6.

[60] F. Jin, X. Li, R. Zhang, C. Dong, and L. Hanzo, "Resource Allocation Under Delay-Guarantee Constraints for Visible-Light Communication," *IEEE Access*, vol. 4, pp. 7301–7312, 2016.

[61] L. Wei, H. Zhang, and B. Yu, "Optimal bit-and-power allocation algorithm for VLC-OFDM system," *Electronics Letters*, vol. 52, no. 12, pp. 1036–1037, 2016.

[62] S. Zhengguo, Z. Yijun, and Z. Yanyu, "The DMT-Based Bit-Power Allocation Algorithms in the Visible Light Communication," in *2012 Second International*

Conference on Business Computing and Global Informatization, Oct 2012, pp. 572–575.

[63] M. Dai, S. Zhang, B. Chen, X. Lin, and H. Wang, "A Refined Convergence Condition for Iterative Waterfilling Algorithm," *IEEE Communications Letters*, vol. 18, no. 2, pp. 269–272, Feb 2014.

[64] A. R. Ndjiongue, H. C. Ferreira, J. Song, F. Yang, and L. Cheng, "Hybrid PLC-VLC channel model and spectral estimation using a nonparametric approach," *Transactions on Emerging Telecommunications Technologies*, vol. 28, no. 12, 2017. [Online]. Available: https://doi.org/10.1002/ett.3224

[65] M. Chiani, D. Dardari, and M. K. Simon, "New exponential bounds and approximations for the computation of error probability in fading channels," *IEEE Transactions on Wireless Communications*, vol. 2, no. 4, pp. 840–845, Jul 2003.

[66] Y. Chen and N. C. Beaulieu, "A simple polynomial approximation to the gaussian Q-function and its application," *IEEE Communications Letters*, vol. 13, no. 2, pp. 124–126, Feb 2009.

[67] S. Rajagopal, R. D. Roberts, and S. Lim, "IEEE 802.15.7 visible light communication: modulation schemes and dimming support," *IEEE Communications Magazine*, vol. 50, no. 3, pp. 72–82, Mar 2012.

[68] J. Antoniou and A. Pitsillides, *Game Theory in Communication Networks: Cooperative Resolution of Interactive Networking Scenarios*. CRC Press, 2013, ISBN 978-1-4398-4808-1.

[69] K. Ifeh, "Transmit-Power Control for Cognitive Radio Networks: Challenges, Requirements and Options," Master's thesis, School of Electrical and Information Engineering, University of the Witwatersrand, Johannesburg, 1 Jan Smuts Ave. Braamfontein, 2050, South Africa, 2012.

[70] M. Felegyhazi and J.-P. Hubaux, "Game Theory in Wireless Networks: A Tutorial," Jan 2006.

[71] J. F. Nash, "Equilibrium Points in N-Person Games," *Proceedings of the National Academy of Sciences of the United States of America*, vol. 36, no. 1, pp. 48–49, 1950.

[72] J. Nash, "Non-cooperative Games," *Annals of Mathematics*, vol. 54, no. 2, pp. 286–295, 1951.

[73] V. Shah, N. B. Mandayam, and D. J. Goodman, "Power control for wireless data based on utility and pricing," in *Ninth IEEE International Symposium on Personal, Indoor and Mobile Radio Communications (Cat. No.98TH8361)*, vol. 3, Sept 1998, pp. 1427–1432 vol.3.

[74] A. Greenwald, A. Jafari, and C. Marks, "No - Regret: A Connection between Computational Learning Theory and Game Theory." *Synthese Library*, vol. 353, pp. 119–140, 2011.

[75] S. Haykin, "Cognitive radio: brain-empowered wireless communications," *IEEE Journal on Selected Areas in Communications*, vol. 23, no. 2, pp. 201–220, Feb 2005.